AD-A085 357 CIVIL ENGINEERING LAB (NAVY) PORT HUENEME CA F/G 13/3
FIBERGLASS-REINFORCED PLASTIC SURFACING FOR RAPID RUNWAY REPAIR--ETC(U)
OCT 79 P S SPRINGSTON

UNCLASSIFIED CEL-TN-1563 NL

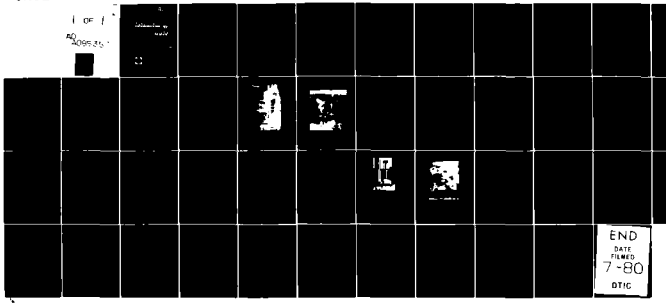

LEVEL II 12

AD A085357

Technical Note

CEL

TN no. N-1563

title: FIBERGLASS-REINFORCED PLASTIC SURFACING FOR RAPID RUNWAY REPAIR BY NAVAL CONSTRUCTION FORCES

author: P. S. Springston

date: October 1979

sponsor: Naval Facilities Engineering Command

program nos: YF53.536.091.01.003E

CIVIL ENGINEERING LABORATORY
NAVAL CONSTRUCTION BATTALION CENTER
Port Hueneme, California 93043

Unclassified

SECURITY CLASSIFICATION OF THIS PAGE (When Data Entered)

REPORT DOCUMENTATION PAGE

READ INSTRUCTIONS BEFORE COMPLETING FORM

1. REPORT NUMBER: TN-1563	2. GOVT ACCESSION NO: DN244122 - AD-A085 357
3. RECIPIENT'S CATALOG NUMBER	
4. TITLE (and Subtitle): FIBERGLASS-REINFORCED PLASTIC SURFACING FOR RAPID RUNWAY REPAIR BY NAVAL CONSTRUCTION FORCES	5. TYPE OF REPORT & PERIOD COVERED: Interim; Nov 78 - Apr 79
	6. PERFORMING ORG. REPORT NUMBER
7. AUTHOR(s): P. S. Springston	8. CONTRACT OR GRANT NUMBER(s): 16 F535 6
9. PERFORMING ORGANIZATION NAME AND ADDRESS: CIVIL ENGINEERING LABORATORY, Naval Construction Battalion Center, Port Hueneme, California 93043	10. PROGRAM ELEMENT, PROJECT, TASK AREA & WORK UNIT NUMBERS: YF53.536.091.01.003E
11. CONTROLLING OFFICE NAME AND ADDRESS: Naval Facilities Engineering Command, Alexandria, Virginia 22332	12. REPORT DATE: October 1979
	13. NUMBER OF PAGES: 46
14. MONITORING AGENCY NAME & ADDRESS(if different from Controlling Office)	15. SECURITY CLASS (of this report): Unclassified
	15a. DECLASSIFICATION DOWNGRADING SCHEDULE

16. DISTRIBUTION STATEMENT (of this Report)

Approved for public release; distribution unlimited.

17. DISTRIBUTION STATEMENT (of the abstract entered in Block 20, if different from Report)

18. SUPPLEMENTARY NOTES

19. KEY WORDS (Continue on reverse side if necessary and identify by block number)

Rapid runway repair, bomb damage repair, airfield pavement repair.

20. ABSTRACT (Continue on reverse side if necessary and identify by block number)

This report documents exploratory research conducted to develop a preliminary concept for repairing bomb-damaged runways with prefabricated fiberglass-reinforced plastic membranes. The membranes would function as traffickable caps over backfilled craters. A structural analysis has been completed using the finite element method and a design is presented for a membrane to be traffic-tested under simulated F-4 aircraft wheel loads at the Rapid Runway Repair Test Facility of the Air Force Engineering and Services

continued

DD FORM 1 JAN 73 1473 EDITION OF 1 NOV 65 IS OBSOLETE

Unclassified

SECURITY CLASSIFICATION OF THIS PAGE (When Data Entered)

20. Continued

Center/Research Division at Tyndall AFB, Florida. Methods for joining panels to form large membranes and a tiedown method are discussed. A general concept for rapid runway repair by the Naval Construction Forces using table-of-allowance (P25 and P31) equipment is presented.

Library Card

Civil Engineering Laboratory
FIBERGLASS-REINFORCED PLASTIC SURFACING FOR RAPID RUNWAY REPAIR BY NAVAL CONSTRUCTION FORCES,
by P. S. Springston
TN-1563 46 pp illus October 1979 Unclassified

1. Rapid runway repair 2. Airfield pavement repair I. YF53.536.091.01.003E

This report documents exploratory research conducted to develop a preliminary concept for repairing bomb-damaged runways with prefabricated fiberglass-reinforced plastic membranes. The membranes would function as traffickable caps over backfilled craters. A structural analysis has been completed using the finite element method and a design is presented for a membrane to be traffic-tested under simulated F-4 aircraft wheel loads at the Rapid Runway Repair Test Facility of the Air Force Engineering and Services Center/Research Division at Tyndall AFB, Florida. Methods for joining panels to form large membranes and a tiedown method are discussed. A general concept for rapid runway repair by the Naval Construction Forces using table-of-allowance (P25 and P31) equipment is presented.

CONTENTS

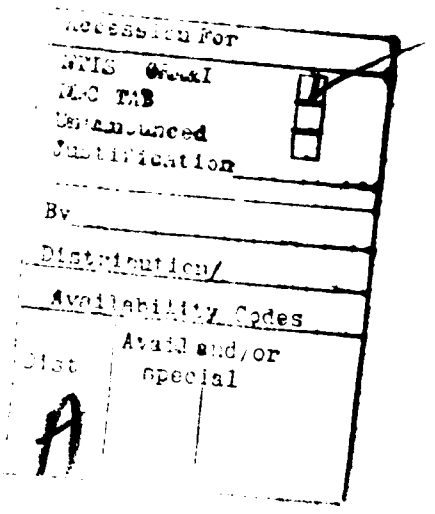

INTRODUCTION AND BACKGROUND

Recent developments have dictated that Naval Construction Forces (NCF)* will be assigned post-attack rehabilitation of Navy/MarCorps** airfield pavements in certain potential theatres of operation. The NCF is capable of accomplishing such a mission from the standpoint of having trained operators and equipment, but the NCF does not have a detailed repair method tailored specifically to its capabilities and equipment assets. In the interest of economy and of quickly developing a Navy Rapid Runway Repair (RRR) capability, the NCF tentatively has adopted the repair methodology developed by the Air Force.

Currently, a time constraint set by the Air Force requires the identification and rehabilitation of a 50-foot by 5,000-foot runway to standards suitable for operation of aircraft within 4 hours after attack. Using three equipment/crew teams, repair of three craters produced by 750-pound bombs should be completed within 4 hours (Ref 1). The Air Force procedure is to remove all broken pavement, backfill the crater with broken pavement and crater ejecta to within 12 inches of the original pavement surface, and fill that upper 12 inches with compacted select base material previously stockpiled. The compacted select base material is brought up to the grade of the original pavement. AM-2 airfield landing mat is assembled on undamaged pavement near the crater and dragged over the filled crater after compaction has been completed. The Air Force currently is studying effects upon aircraft of roughness induced by high-speed transitions from pavement to surface mounted matting (1.5-inch bump height). Some critical combinations of spacing and ground speed may be deleterious to aircraft carrying external stores of munitions or wing-tip fuel tanks. This report documents the preliminary development of an alternative concept to AM-2 matting for a bomb crater cap - a fiberglass-reinforced plastic (FRP) membrane. Such a membrane would be relatively thin and would, in effect, be a flush-mounted cap.

Southwest Research Institute (SWRI) under contract to the Air Force Engineering and Services Center (AFESC) has recommended numerous rapid runway repair (RRR) concepts for further study (Ref 2). One of these concepts entails a bomb crater backfilled with debris and ejecta, topped with sand, and covered with an FRP membrane as a traffickable surface. The Civil Engineering Laboratory (CEL) has conducted and supervised considerable research in the use of FRP as an expedient beach and roadway

*Seabees.
**Marine Corps.

surfacing material for vehicular traffic (Ref 3,4,5,6). The chemicals and spray equipment have become known as the Advanced Multipurpose Surfacing System (AMSS). The AMSS equipment consists of trailer-mounted hardware for pumping and blending polyester resin, a promoter, and a catalyst (Figure 1). The polyester resin is spray-applied with a hand-held spray gun (Figure 2). The hardware is currently being re-configured by CEL for the MarCorps to achieve compatibility with a containerized shipping mode.

OBJECTIVE

This report documents exploratory research conducted to develop a preliminary concept for RRR utilizing (1) the AMSS materials and equipment for construction of a traffickable crater cap and (2) organic NCF equipment for backfill and compaction of craters. The objective is to tailor the concept to existing NCF and MarCorps equipment resources. A test plan (Ref 7) has been developed for the traffic testing of the concept by a simulated F-4 aircraft wheel load (267-psi tire pressure and 27,000-lb single wheel load) during August 1979. The concept will be tested at a permanent facility for RRR testing at Tyndall AFB, Fla. (see Appendix A for discussion of the test facility). This report develops and evaluates the RRR concept with respect to soils and load conditions which will be encountered during traffic testing of repaired simulated craters at Tyndall AFB. Effort was not expended to extrapolate analytical conclusions to the many variables (crater types and sizes, soil types, etc.) that would be present in an actual crater repair problem.

APPROACH

Concept development was divided into four segments - (1) design of membrane thickness, (2) investigation of methods for joining membranes, (3) cursory investigation of tiedown methods to anchor an FRP crater cap to existing pavement, and (4) proposal of a viable general concept of RRR with FRP membranes. Laboratory experiments were conducted to determine tensile strength and elastic modulus values for the 5-year shelf life polyester resin RS 50338, developed by the Dow Chemical Company (Ref 5). The modulus value was then used as input to a finite element computer program, SLIP (Ref 8), to analyze the effects on membrane stresses and displacements of varying backfill soils and membrane thicknesses; and, ultimately, an optimum membrane thickness and backfill were selected.

In the joining study, several panels were manufactured and joined, using polyester resin as an adhesive. The original intent was to join prefabricated FRP panels by overlapping bare fiberglass edges and saturating them with polyester resin which, when cured, was to provide a

permanent bond between panels. Samples for tension testing were cut from cured panels and tested to determine failure mode and ultimate tensile strength of the joints. As a result of these tests further work on joining methods was recommended.

The suitability of several types of commercially available fasteners for tiedown of an FRP crater cap was evaluated and a preliminary method was suggested. A small 1/2-inch x 5-foot x 12-foot panel was manufactured and used to test the feasibility of using the fasteners to anchor the cap to a Portland cement concrete pavement. Bolts driven by powder-actuated tools as well as various types of rock bolts were investigated.

After determination of membrane thickness and preliminary study of joining methods, a general concept for RRR with FRP membranes was originated. The proposed concept utilized equipment currently listed in Naval Construction Force equipment allowances.

MEMBRANE THICKNESS DESIGN

Finite element computer code SLIP, developed by E. L. Wilson of the University of California and later modified by CEL, was used to evaluate the effects of membrane thickness on membrane displacements and stresses. In general, SLIP models a pavement system as an axisymmetric solid (layered conical frustrum) and is based upon elastic layered assumptions with solution by the finite element technique. Infinitely small strain, small displacement theory, and linear elastic material response are assumed. Although the latter assumption is not entirely valid with respect to the soil response for the RRR concept, the program was deemed to be valuable for prediction of the relative responses of the soil-FRP membrane system when various design options were considered (e.g., increasing membrane thickness versus adding a compacted base course).

A repair profile of FRP over a clay subgrade (Figure 3) was first analyzed. The subgrade was considered as being linear elastic with an estimated Young's modulus of 6,000 psi. The program was flagged to permit tangential slip at the membrane-soil interface and to solve for boundaries free at an angle of 30 degrees to the vertical. F-4 aircraft wheel load was input as a pressure loading of 267 psi over a 5.67-inch radius. Total system (soil and membrane) depth was fixed at 15 load radii, and width was held constant at 6 radii. The number of radial elements was increased in successive approximations from 11 (mesh no. 1) to 17 (mesh no. 4) to test for solution convergence. Convergence was observed by mesh no. 4 for deflection, strain (Figure 4), and stress. One additional solution was performed (mesh no. 5), which added one row of elements for a total of four rows to the membrane mesh. Calculated values for mesh no. 5 agreed very closely with those for mesh no. 4 and all succeeding solutions utilized mesh no. 5 (Figure 5).

Having selected a mesh which satisfied convergence criteria, solutions were performed for membranes having thicknesses of 1/2, 5/8, and 3/4 inch. Plots of predicted displacements revealed marginal distinction

between the deflection basins for the three membranes (Figure 6); furthermore, membrane stresses were approximately equal. Increasing membrane thickness was not, therefore, an effective way of improving performance. The effect of a stronger soil layer below the membrane was next investigated.

The idealized repair profile consisted of a 0.5-inch FRP membrane placed on 12 inches of crushed stone (estimated E = 20,000 psi) overlying 6 feet of clay (estimated E = 6,000 psi). Analysis indicated that the relatively stiff layer of crushed stone would distribute wheel load stresses, thereby reducing membrane deflection (eventual rutting) and lowering membrane stresses (2,379 psi versus 5,639 psi for a 0.75-inch membrane over clay). Addition of a stiff soil layer beneath the membrane was considered, therefore, to be more cost-effective toward improving performance than increasing membrane thickness. The minimum membrane thickness was judged, arbitrarily, to be 0.5 inch with the fundamental consideration being to insure sufficient thickness to prevent puncture of the FRP from particles of the crushed stone base.

To predict soil-membrane response more accurately, close estimates of Young's modulus for the base course and clay were required. Initially, the moduli were estimated as being 20,000 psi and 6,000 psi for the crushed stone and clay, respectively. A solution by SLIP for a 1/2-in.-thick membrane over 12 inches of crushed stone underlain by clay predicted normal stresses beneath the load center at a depth of one load radius (within the crushed stone base course) to be -151.4 psi (vertical)* and -7.8 psi (lateral).** For the first element row within the clay layer, the predicted normal stresses were -39.7 psi (vertical) and -0.6 psi (lateral). Triaxial tests were conducted to determine the response characteristics and representative moduli for the clay and crushed stone materials at these stress states. Test procedures and material response curves are included in Appendix B.

An iterative procedure was followed whereby the predicted soil stress state was located on the appropriate soil stress-strain curve and the elastic modulus was computed at that point, using the secant method. The new modulus was then input to the computer program and the code re-run. This sequence was iterated until experimental moduli and stress states (curves) matched those for the representative elements of the SLIP crater model. During the soil testing and computer analyses, the stone and clay soils were found to be weaker (lower elastic moduli) than originally estimated. Consequently, the depth of the stone layer was increased to a thickness of 24 inches. The final idealized crater profile is depicted in Figure 7. The degree of matching between the analytical and experimental soil stress states used to characterize the

*A negative sign convention is used to represent compressive stress.

**Analyses of full-scale load tests conducted by CEL have indicated that, for loads placed directly on dense sand and clay subgrades, the stress state which appeared to be representative of the average state for the subgrade was that located at a depth of one load radius beneath the load center (Ref 9).

material models for analysis can be determined from Table 1. The final predicted stress states were marked on the material response curves (Figures 8 and 9). From Figures 8 and 9 it should be noted that the original assumption of linear-elastic soil behavior was not seriously in error as the material responses at the given stress levels are approximately linear elastic. The soil preparation and test methods are discussed in Appendix B.

The final estimate of initial static deflection beneath the F-4 wheel load is 0.25 inch and the deflection profile is depicted in Figure 10. The predicted soil-strain distribution is plotted in Figure 11. The predicted initial static deflection and soil strains will be compared with data which will be recorded during the August 1979 traffic testing at Tyndall AFB (Ref 7). The analysis indicates that the crushed stone base course material reaches or approaches yield and will be close to failure (Figure 9). Two alternative responses are possible when subjected to the wheel load - (1) the base course may fail through rutting or (2) the base course may be further densified with a resultant strength increase. To insure the latter response, it is recommended that a filter-fabric-type membrane be placed at the stone base course and clay interface. A single layer of 4020* fiberglass mat incompletely saturated ("starved") with polyester resin would be a suitable membrane. The material cost for a 0.5-inch FRP cap with such a filter membrane is estimated to be $5.00/sq ft (1979).

MEMBRANE JOINING

Conceptually, large FRP panels (>400 sq ft) could be fabricated by military personnel and pre-positioned near the areas of intended use. The panels could be dragged to a repair site by a crawler tractor or other vehicle with suitable drawbar pulling power. A rapid method of structurally joining several panels to form a single membrane - transfer of tensile stress - may be required, however.

Several joining methods were considered - mechanical fastening, adhesive bonding, and a combination of both. Mechanical fastening with blind rivets, bolts, or integral devices was deemed to be too time consuming and expensive; moreover such methods would probably result in critical stress concentrations. Adhesive bonding was considered the optimum method. Since the majority of structural adhesives require a relatively long cure time in the absence of elevated temperature, thermosetting polyester resin was selected as a prime candidate.

The selected adhesive joining concept was the formation of a bonded joint by saturation of overlapped fiberglass margins along panel sides with polyester resin (15-minute cure time). Panels would be fabricated with a margin of unsaturated fiberglass along the panel perimeters.

*4020 is a manufacturer's designation which represents 4.4 oz/sq ft woven roving and 2 oz/sq ft random fiber.

Field joining of adjacent panels would be accomplished by (1) overlapping fiberglass edges, (2) placing an additional fiberglass layer across the top of the joint (similar to a splice plate), (3) saturating the fiberglass with polyester resin, (4) rolling the joint to expel trapped air, and (5) curing. Small FRP panels (1/2 x 24 x 40 inches) were manufactured in the laboratory, field-joined, and used to fabricate samples for tension tests, which were conducted to determine the optimum joint configuration and the required overlap.

Prior to joint testing, an FRP panel was manufactured having 4 plies of 4020 fiberglass mat saturated with PPG Industries RS 50338 polyester resin. The purpose of these tests was to quantify the FRP tensile properties. Three samples of 1/2-inch nominal thickness were cut from the panel, instrumented and tested in axial tension parallel to the roving direction. Nominal sample width was 1 inch with a geometry as illustrated in Figure 12. The samples were instrumented with EA-41-250BG-120 strain gages (0.25-inch gage length) affixed with M-Bond Type AE epoxy-adhesive resin.* The panel had been fabricated against a hard, level surface; thus, one side of each sample was essentially smooth. Gages were mounted on the smooth sides of the samples after surface preparation consisting of light sanding with no. 300 grit sandpaper followed by cleaning with isopropyl alcohol. The FRP was found to have an elastic modulus of 1,400,000 ± 125,000 psi and an ultimate tensile strength of 17,290 ± 523 psi. Typical material response is illustrated by Figure 13.

Three joining configurations were investigated, all of which depended upon overlapping and saturation of bare fiberglass panel edges with polyester resin to develop a structural bond (Figures 14 through 16). Small panels (approximately 24 x 24 inches) were manufactured and joined together in the manner described in Figures 14-16. Field fabrication methods were closely simulated. Once two panels were joined and cured, tensile specimens were fabricated from them with a geometry similar to that of Figure 12 except that overall length was 48 inches. Sample widths varied from 2 to 1 inch. The samples were tested in uniaxial tension in a Tinius Olsen universal testing machine (Figure 17).

From Table 2, it is evident that the three joining methods developed nearly comparable tension load transfer. Only tensile specimens without visible flaws were used for testing purposes; thus, even though method C would rank second in effectiveness, it is recommended because of the consistency of the joint. None of the joints were entirely satisfactory since load transfer represented only about 53% of the ultimate load capacity of the parent material. It is noted, however, that analysis predicts that a static tension load transfer of 1,799 lb/in. (Factor of Safety = 1.0) is satisfactory to support the F-4 wheel load.

Joint failure appeared to initiate in the splice plates which debonded. This was followed by debonding of the lapped panel edges, constituting complete failure. Further studies of joining methods are recommended and should focus on effects of increasing the amount of lap and roughening the upper panel surface where the top splice plate is to be applied.

*Product of Micro-Measurements, Romulus, Mich.

PANEL TIEDOWN

A membrane cap would require anchoring to resist (1) deceleration forces produced by braking aircraft and (2) the uplifting effects of jet engine backwash. Preliminary study of the tiedown problem led to a concept utilizing powder-actuated tools to drive bolt-type fasteners into a concrete pavement thereby anchoring a membrane. In a small scale trial, 1/4-in.-diam bolt fasteners (Figure 18), manufactured by the Hilti Co., were used to anchor a 1/2-inch x 5-foot x 12-foot FRP membrane (Figure 19). Holes of 1/2-inch diameter were pre-drilled in the membrane with a carbide-tipped masonry drill bit at the rate of 6 holes/min, and the fasteners were driven with a Hilti Model DX600 gun at a rate of 1 min/fastener. The pullout strength of the powder-driven fasteners was found to be low as a fastener could be withdrawn from the concrete by application of torque to the fastener nut. Powder-driven fasteners were thus found to be unsatisfactory for panel tiedown.

Rock bolts next were investigated as tiedown fasteners. Rock bolts develop their anchoring strength by mechanically expanding the down hole end of the bolt thereby developing an anchoring force which is obtained through a combination of friction, adhesion between the anchor and rock, and physical penetration of the anchor into the rock (Ref 10). Rock bolts are commercially available in a variety of forms which may be generally classified into two types: (1) drive-set and (2) torque-set. A successful installation of the drive-set type of fastener depends on accurately drilling the hole to a predetermined depth and on applying sufficient force to completely expand the slotted rod. This type of fastener was tried and found to be unsatisfactory - gaging hole depth was time-consuming, and the fasteners were pulled from the concrete upon application of torque.

A torque-set bolt is shown in Figure 20. This type of fastener has a wedge or cone which is threaded to the bottom of the bolt or, as in Figure 20, is an integral part of the threaded stud. A sleeve is pushed into the hole with the bolt and surrounds the cone. Once the bolt has been inserted, torque is applied to the nut to cause the bolt and cone to be pulled up through the sleeve, thus securing the anchorage. The torque-set type of bolt was found to require far less precision in hole drilling as long as the depth of the hole was greater than the length of the bolt.

Torque-set bolts are recommended for panel tiedown. Those tested and found satisfactory were 1/2- x 3-inch Lok/Bolts manufactured by the Rawlplug Co. of New Rochelle, N.Y.* When installed in 1/2-in.-diam pre-drilled holes in 3,000-psi compressive strength concrete, the ultimate tensile strength of the bolt was developed. Holes of 1/2-inch diameter were drilled in the concrete at a rate of four holes/min using a Rockwell rotary hammer (drill). Fastener setting required an additional 25 sec/bolt (an impact wrench would considerably reduce this time). Holes of 3/4-inch diameter were drilled in the FRP at a rate of

*No other manufacturer's torque-set bolts were tested.

15 sec/hole. These could possibly be drilled along the perimeter of panels during fabrication, thus eliminating FRP hole drilling during the critical crater repair.

An analysis of bolt spacing requirements was not attempted. However, a bolt spacing of 4 feet on-center along the membrane perimeter is estimated to be sufficient. The FRP would be drilled with a larger hole than the tiedown bolt diameter (3/4-inch for a 5/16-inch bolt) to permit thermal expansion and contraction. Fastener installation would require approximately 40 seconds total time per bolt per two-man team. Further study is recommended to define optimum fastener spacing and fastener effectiveness.

GENERAL CONCEPT

FRP membranes having a thickness of 1/2 inch and a plan dimension of approximately 20 x 70 feet could be prefabricated by military personnel having minimal training and low skill level and using existing MARCORPS equipment. The membranes could be staged near their intended use areas at airfields (e.g., shallow-buried in an infield or stored in a hardened shelter). After an attack and subsequent ordnance clearing, ejecta would be shoved into craters and uplifted pavement sections would be removed. A filter fabric of 4020-weight fiberglass mat next would be spread over the backfilled debris and incompletely saturated with spray-applied polyester resin, utilizing the AMSS equipment and chemicals. Concurrently with installation of the filter fabric, equipment would top off the crater with crushed stone base course material conforming to ASTM Test Designation D-2940 (Ref 11). This base material would be compacted by a total of 32 coverages with a vibratory roller having a compactive effort of at least 27,000 pounds of dynamic force at 1,100 to 1,500 vpm with a total applied force of 44,900 pounds. Panels would be towed from storage by equipment having suitable drawbar pull (approximately 3,500 to 7,000 pounds). Panels would be delivered to a clear area on the runway adjacent to the crater, positioned, and joined to form a membrane cap. Upon completion of compaction and grading of the crushed stone, the assembled cap would be towed across the crater and fastened to the pavement with masonry bolts; thus, the membrane can be rapidly removed and refastened to permit reworking of the crater fill material to smooth ruts which develop from prolonged trafficking.

A flow network based on the critical path method was drafted to illustrate the interrelationships of the various activities (Figure 21) associated with the repair of a single 750-pound bomb crater (Figure 22) by a single crew/equipment team. The repair included the replacement of 290 loose cu yd of ejecta, and the placement of 255 compacted cu yd (500 tons) of crushed stone base course material. The critical path includes the replacement of debris and the loading and 1-mile round-trip hauling of stockpiled base material to the repair site. To constrain repair time within acceptable limits, large augment-P31*-equipment items

*P31 Construction Equipment Allowance of the Advanced Base Functional Component System.

are required. Figure 21 depicts equipment assignments by activity. Activity time estimates were derived through use of standard equipment production formulas using an efficiency of 0.75. The estimate for the removal of uplifted pavement was more subjective, and therefore the weakest of the activity estimates. Removal rates for large pavement chunks would be highly dependent on many variables, including operator skill level, type and thickness of pavement, and weather (equipment traction). It should be noted that a single equipment/crew team could repair multiple craters at a faster rate than for a single crater since there would be overlap in the critical paths; furthermore, surveying and mobilization are nonrecurring activities.

CONCLUSIONS AND RECOMMENDATIONS

With respect to an analysis of static load conditions represented by the takeoff main gear load of an F-4 aircraft, a 1/2-in.-thick fiberglass-reinforced polyester resin membrane is feasible as a trafficable cap over a backfilled and compacted runway crater. A minimum of 24 inches of crushed stone base compacted at or slightly below optimum moisture content (Ref 12) should underlie the membrane and should be separated from the crater debris (clay in the case of a traffic test at Tyndall AFB) by a filter fabric. The filter fabric should be incompletely saturated with polyester resin and should contain 40 oz/sq yd of woven fiberglass. Further study is required to more fully define methods of joining panels and membrane tiedown. Also, dynamic effects produced by the taxiing and braking of aircraft on the membrane should be investigated. Traffic life of the membrane under a quasi-static load represented by an F-4 aircraft main gear wheel (27,000 pounds and 267 psi) should be determined. The stated crushed stone depth is considered a minimum figure and the membrane may fail during traffic testing through excessive roughness (rutting). Edge effects produced by moving wheel loads transitioning from a rigid existing pavement to the flexible membrane were not investigated.

ACKNOWLEDGMENTS

The assistance of Mr. George Wu, Civil Engineer, who conducted the triaxial soil testing and Mr. Leonard Woloszynski, Civil Engineering Technician, who conducted all other materials testing is gratefully acknowledged. Both gentlemen are members of the Soils and Pavements Division of the Civil Engineering Laboratory.

REFERENCES

1. Department of the Air Force. AFR 93-2: Disaster preparedness and base recovery planning. Washington, D.C., Jul 1974.

2. Civil and Environmental Engineering Development Office. Contractor review conference, Tyndall Air Force Base, Fla., 1-2 Jun 1978.

3. Civil Engineering Laboratory. Technical Note N-1346: Evaluation of a synthetic surfacing system for the Marine Corps, by D. F. Griffin. Port Hueneme, Calif., Jul 1974.

4. _____. Technical Memorandum M-53-76-1: Fiberglass reinforced polyester performance under dual wheel traffic loadings, by M. C. Hironaka. Port Hueneme, Calif., Jan 1976.

5. _____. Contract Report CR 78.018: Fabrication of fiberglass reinforced plastic surfacing under wet conditions. Dow Chemical Company, Walnut Creek, Calif., Sep 1978.

6. _____. Contract Report CR 77.017: Improved chemical components for formulating fiberglass-reinforced plastic soil surfacing. Dow Chemical Company, Walnut Creek, Calif., May 1977.

7. _____. Technical Memorandum M-53-79-3: Test plan for traffic testing of an expedient airfield pavement and a rapid runway repair concept, by P. S. Springston and M. McNerney, Capt., USAF (AFESC). Port Hueneme, Calif., Feb 1979.

8. Naval Civil Engineering Laboratory. Technical Report R-763: Layered pavement systems - Part I. Layered system design; Part II. Fatigue of plain concrete, by J. B. Forrest, M. G. Katona, and D. F. Griffin. Port Hueneme, Calif., Apr 1972.

9. Federal Aviation Administration. Report No. FAA-RD-76-206: Experimental relationships between moduli for soil layers beneath concrete pavements, by J. B. Forrest, P. S. Springston, M. G. Katona, and J. Rollins. Washington, D.C., Jun 1977.

10. Civil Engineering Laboratory. Technical Report R-824: Handheld hydraulic rock drill and seafloor fasteners for use by divers, by R. L. Brackett and A. M. Parisi, LT, CEC, USN. Port Hueneme, Calif., Aug 1975.

11. American Society for Testing and Materials. "Standard specification for graded aggregate material for bases or subbases for highways or airports," 1978 Annual Book of ASTM Standards, Part 14, Philadelphia, Pa., 1978. (Designation D2940-74)

12. _____. "Standard test methods for moisture-density relations of soils using 5.5-lb rammer and 12-in. drop," 1978 Annual Book of ASTM Standards, Part 19, Philadelphia, Pa., 1978. (Designation D698-70)

13. Air Force Engineering and Services Center. Engineering and Services Laboratory Technical Report ESL-TR-79-01: Interim field procedure for bomb damage repair using crushed stone for crater repairs and Silikal for spall repairs, by Michael T. McNerney, Capt., USAF. Tyndall AFB, Fla., Apr 1979.

14. Air Force Engineering and Services Center, Research Division. Rapid runway repair contractor review conference. Tyndall AFB, Fla., Apr 1979.

15. Civil and Environmental Engineering Development Office. Technical Report TR 79-14: Field test of expedient pavement repair. Tyndall AFB, Fla. (In Publication)

16. Air Force Civil Engineering Center. Technical Report TR-75-24: Bomb damage repair and damage prediction, by George W. Brooks, John E. Cunningham, and Paul W. Mayer. Tyndall AFB, Fla., Oct 1975.

17. Department of Defense. Military Standard No. MIL-STD-619B: Unified soil classification system for roads, airfields, embankments and foundations. Washington, D.C., Jun 1968.

18. Civil and Environmental Engineering Development Office. Technical Report TR-78-44: Laboratory evaluation of expedient pavement repair materials, by R. Rollings, Capt., USAF. Tyndall AFB, Fla., Jun 1978.

19. Army Engineer Waterways Experiment Station, Civil Engineering. Miscellaneous Paper No. 5-73-56: Lateral distribution of aircraft traffic, by D. M. Brown and O. O. Thompson. Vicksburg, Miss., Jul 1973.

20. D. E. Daniel and R. E. Olson. "Stress-strain properties of compacted clays," Journal of the Geotechnical Engineering Division, ASCE, vol 100, no. GT10, Oct 1974.

21. R. T. Wong, H. B. Seed, and C. K. Chan. "Cyclic loading liquefaction of gravelly soils," Journal of the Geotechnical Engineering Division, ASCE, vol 101, no. GT6, Jun 1975.

22. D. N. Marachi, C. K. Chan, and H. B. Seed. "Evaluation of properties of rockfill materials," Journal of the Soil Mechanics and Foundations Division, ASCE, vol 98, no. SM1, Jan 1972.

Table 1. Soil Stress States

Item Measured[a]	SLIP Prediction	Experimental Curve
Crushed Stone (z = 5.90 in.)[a]		
E (psi)	12,308 (input)	12,308
σ_z (psi)	-151.9	-151.9
σ_r (psi)	-12.5	-15.0
ε_z (%)	-1.2	-1.2
Clay (z = 25.10 in.)		
E (psi)	1,740 (input)	1,740
σ_z (psi)	-6.5	-6.0
σ_r (psi)	0.9	0.0
ε_z (%)	-0.4	-0.4

[a] z = depth below load surface
σ_z = vertical normal stress
σ_r = radial normal stress
ε_z = vertical (axial) strain
E = elastic (Young's) modulus
(-) = indicates compression

Table 2. Comparison of Joint Effectiveness

Joining Method	Average Failure Load (lb)	Average Sample Width (in.)	Average Load Transfer (lb/in.)
A (Figure 14)	7,867	2.0	3,967
B (Figure 15)	7,540	1.6	4,654
C (Figure 16)	4,440	1.0	4,429

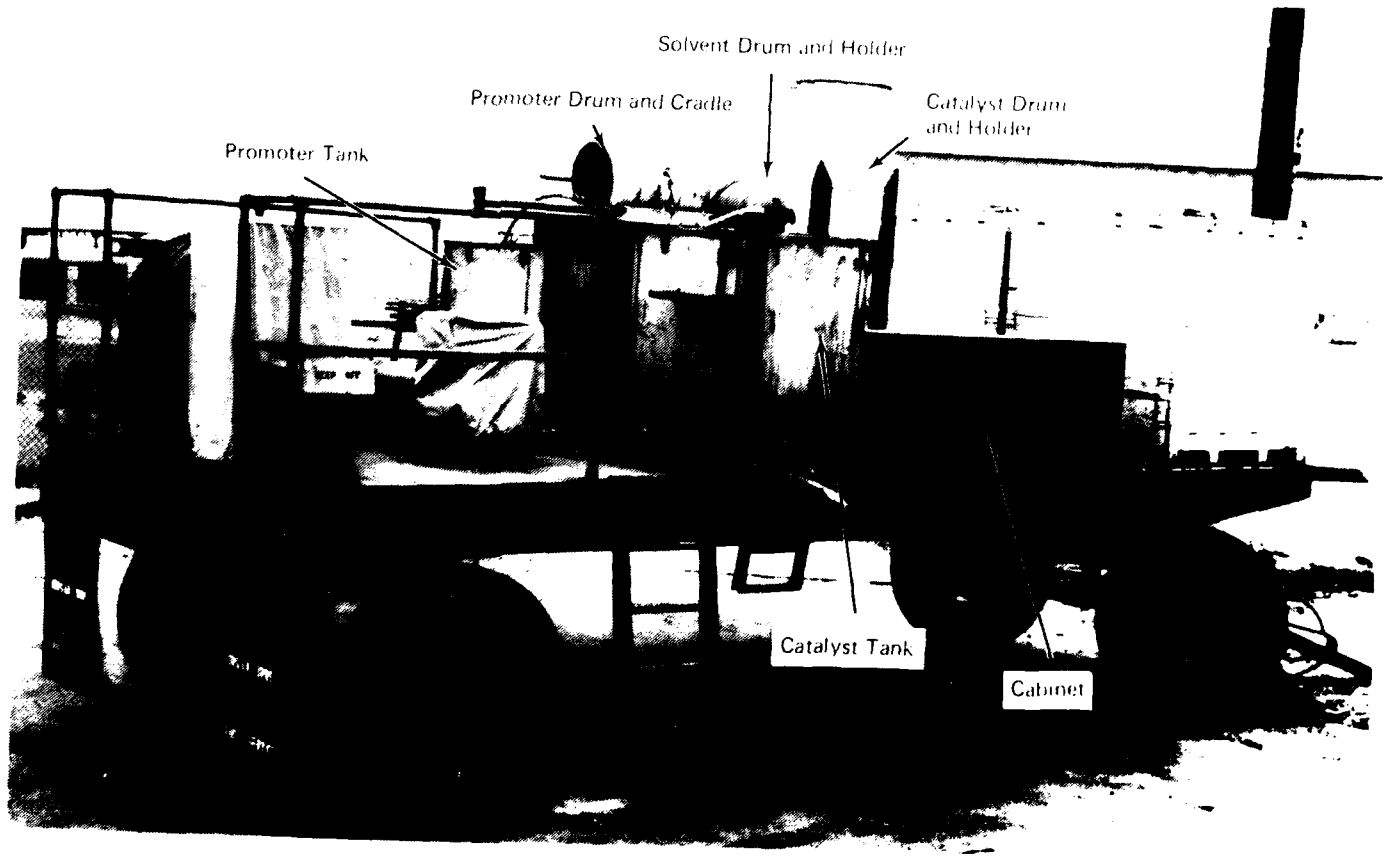

Figure 1. Trailer-mounted spray equipment of the Advanced Multipurpose Surface Sealer.

Figure 2. Spray application of polyester resin to a woven fiberglass.

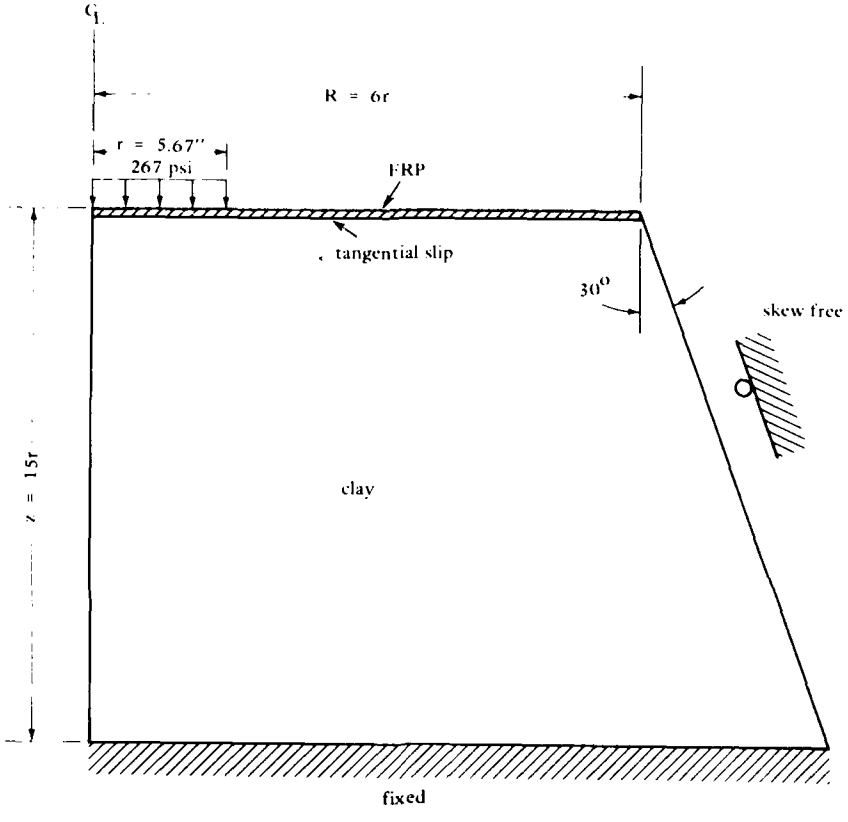

Figure 3. Idealized RRR cross section for convergence testing.

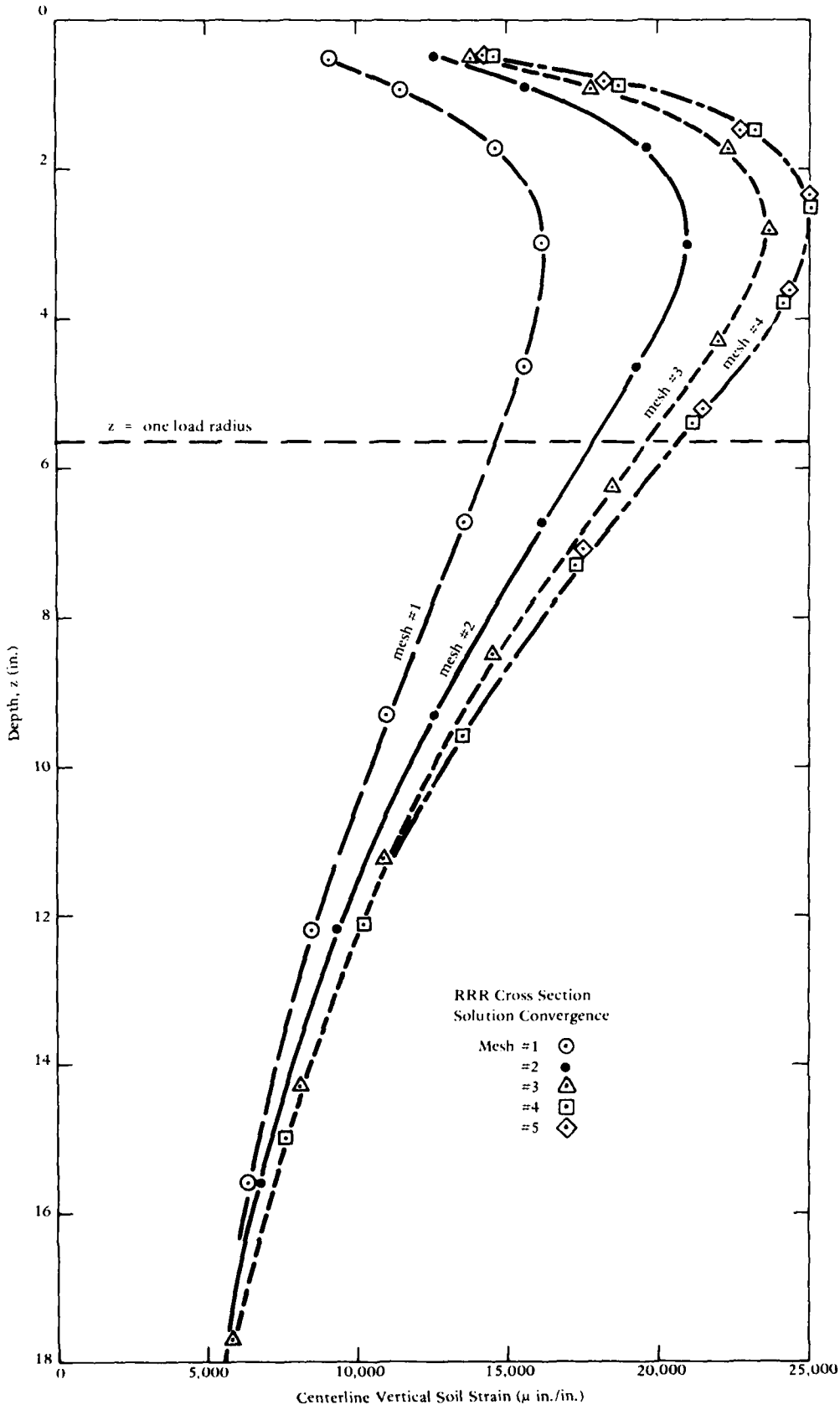

Figure 4. Convergence of soil strain.

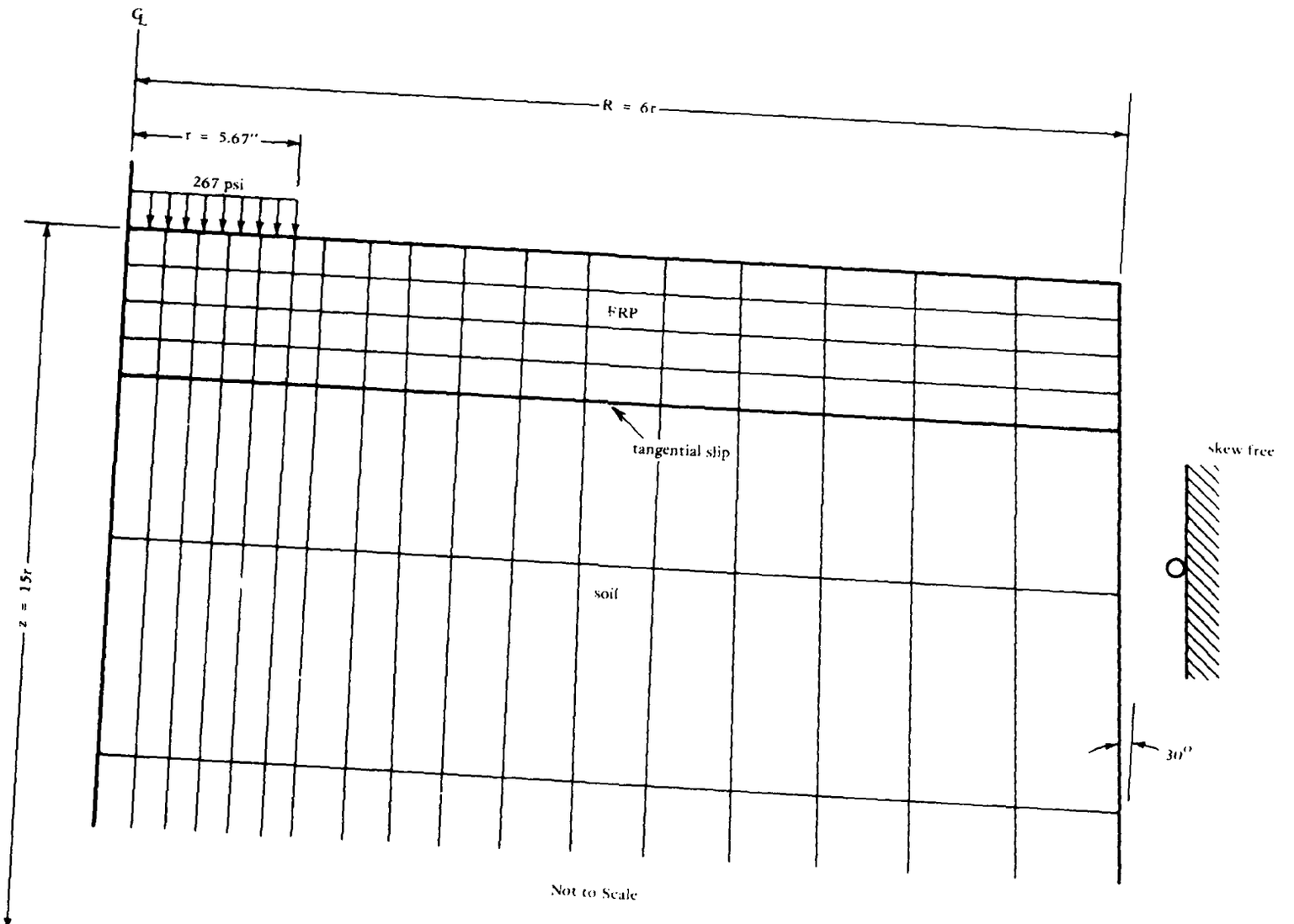

Figure 5. RRR idealization mesh #5.

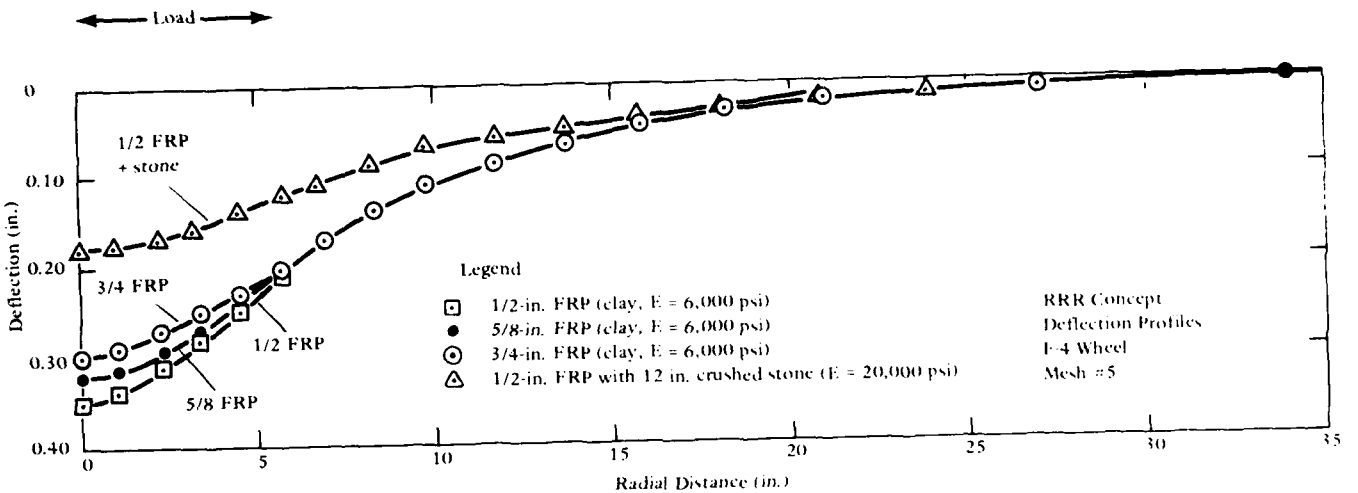

Figure 6. Deflection profiles for FRP membranes under an F-4 static wheel load.

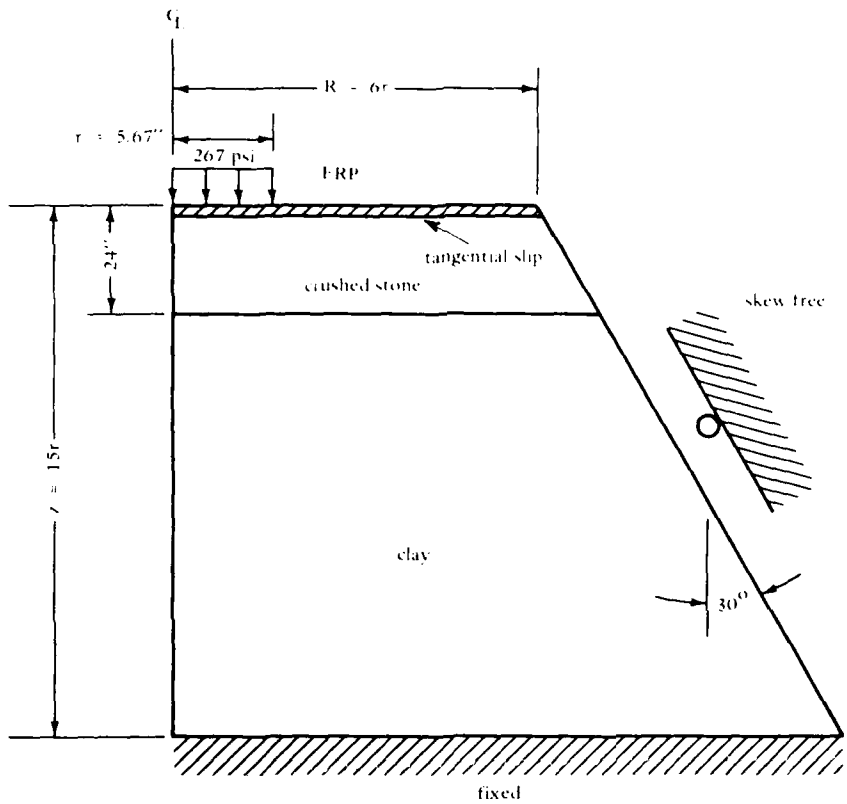

Figure 7. Idealized RRR cross section with crushed stone base.

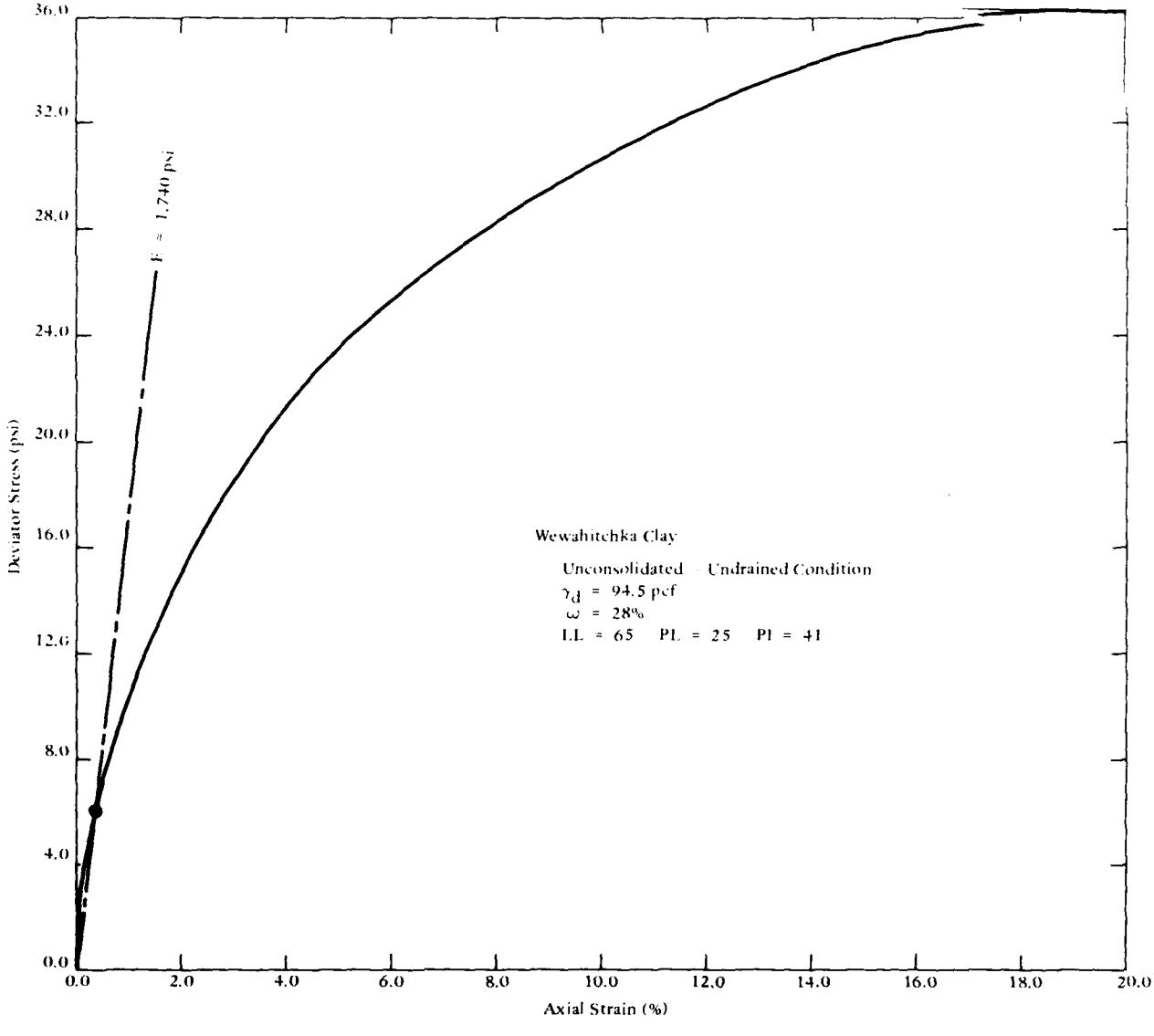

Figure 8. Averaged response for Wewahitchka clay triaxial tested in an unconsolidated-undrained condition.

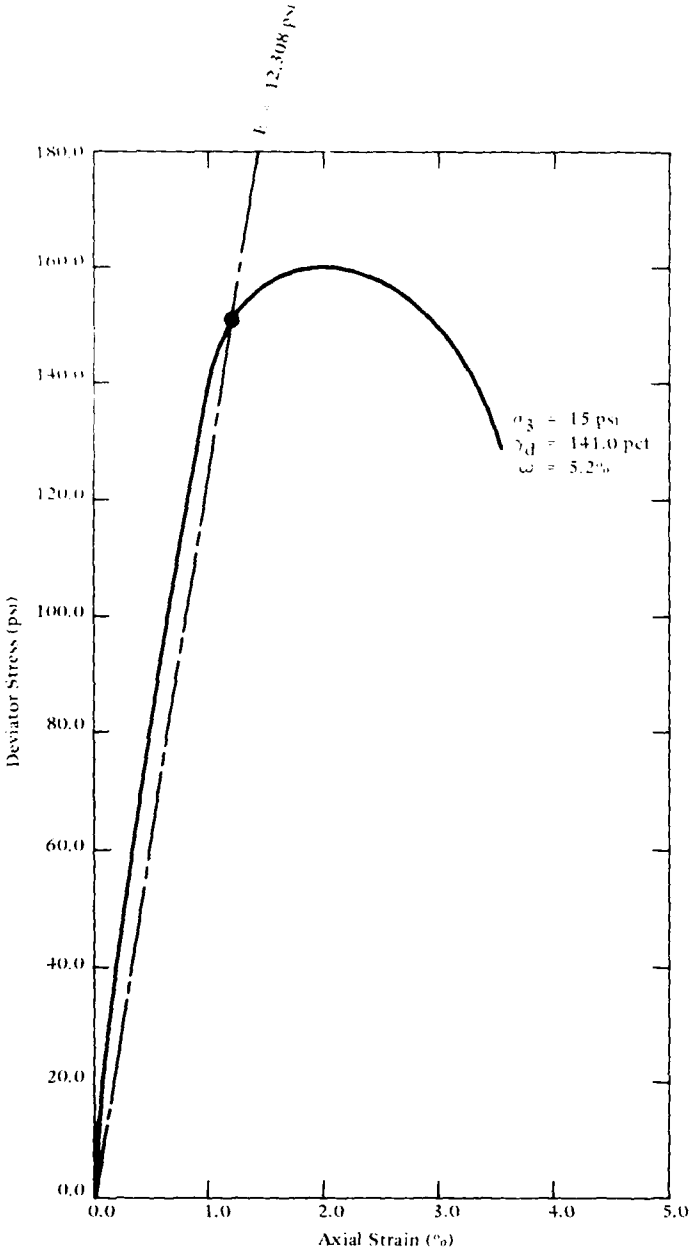

Figure 9. Response of Tyndall crushed stone triaxial tested in a consolidated-drained condition at a 15-psi confining pressure.

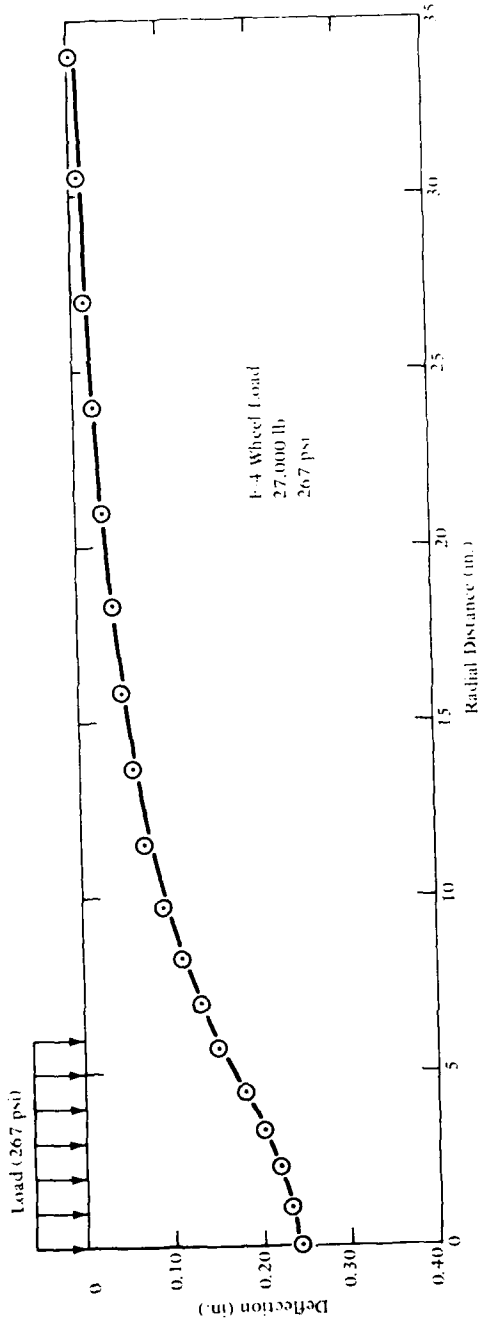

Figure 10. Deflection profile for 12-in. PCC over 24-in. crushed stone base.

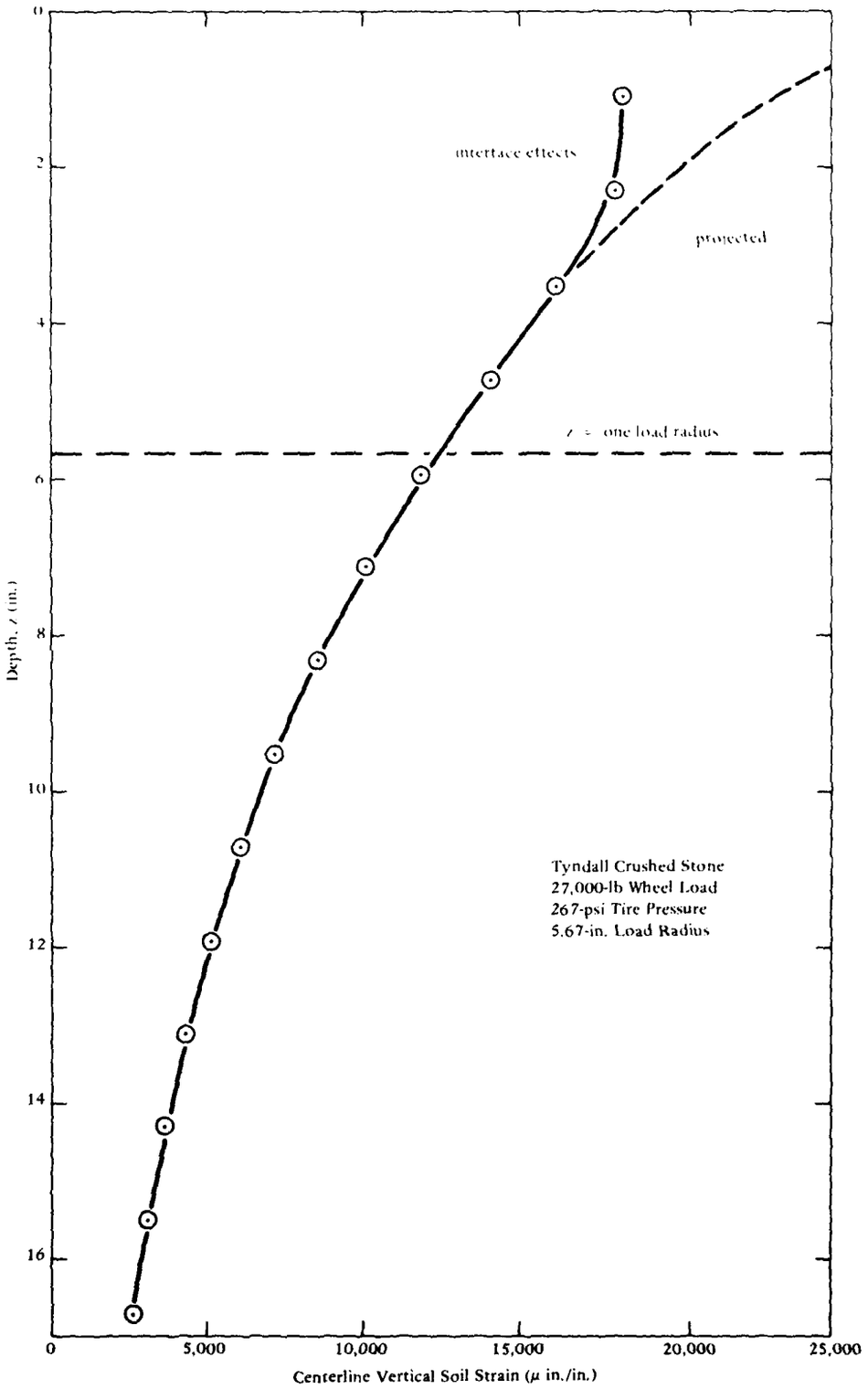

Figure 11. Centerline vertical soil strain for 1/2-in. FRP over 24 in. of crushed stone base.

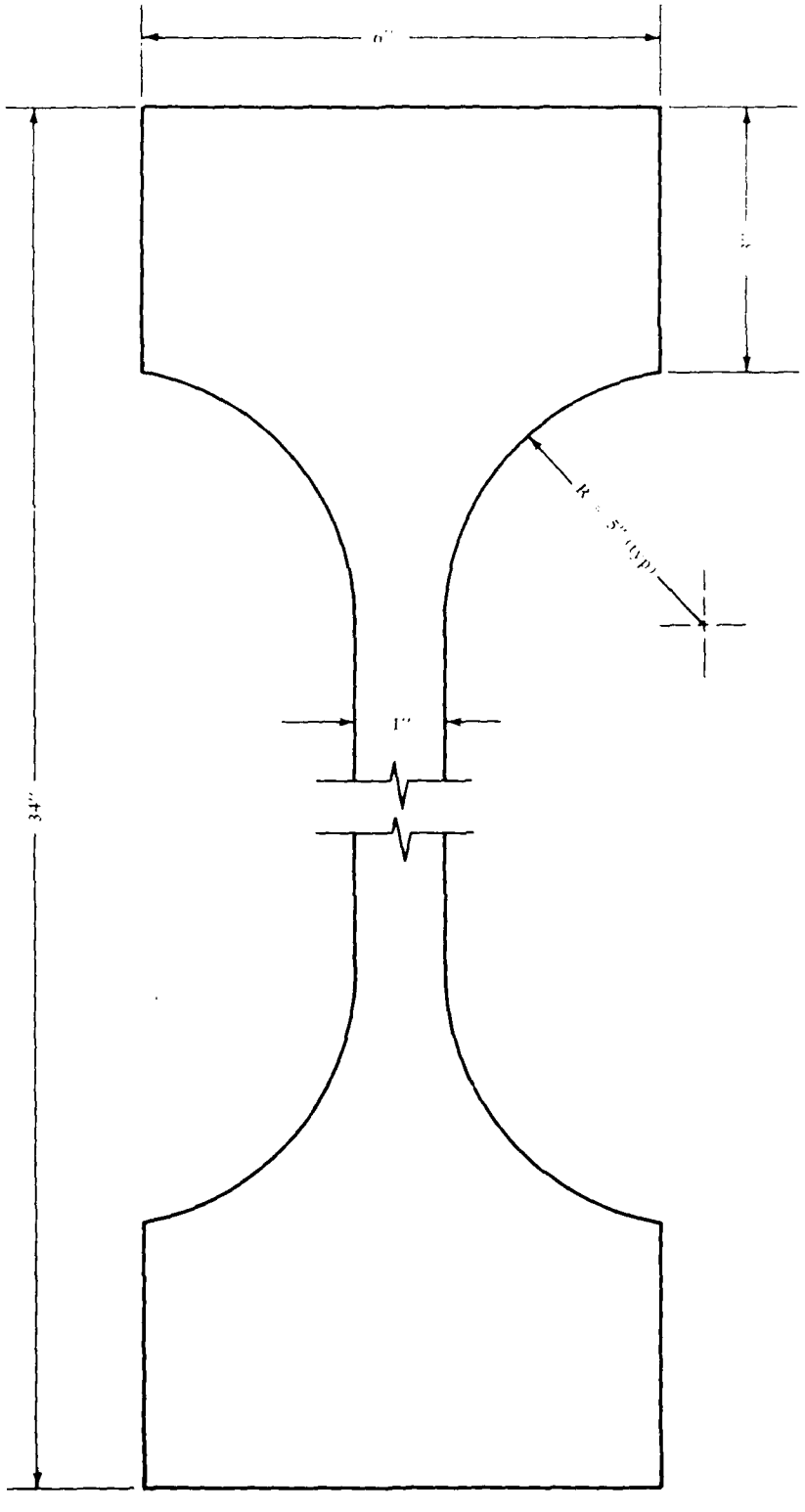

Figure 12. Typical FRP tensile test specimen.

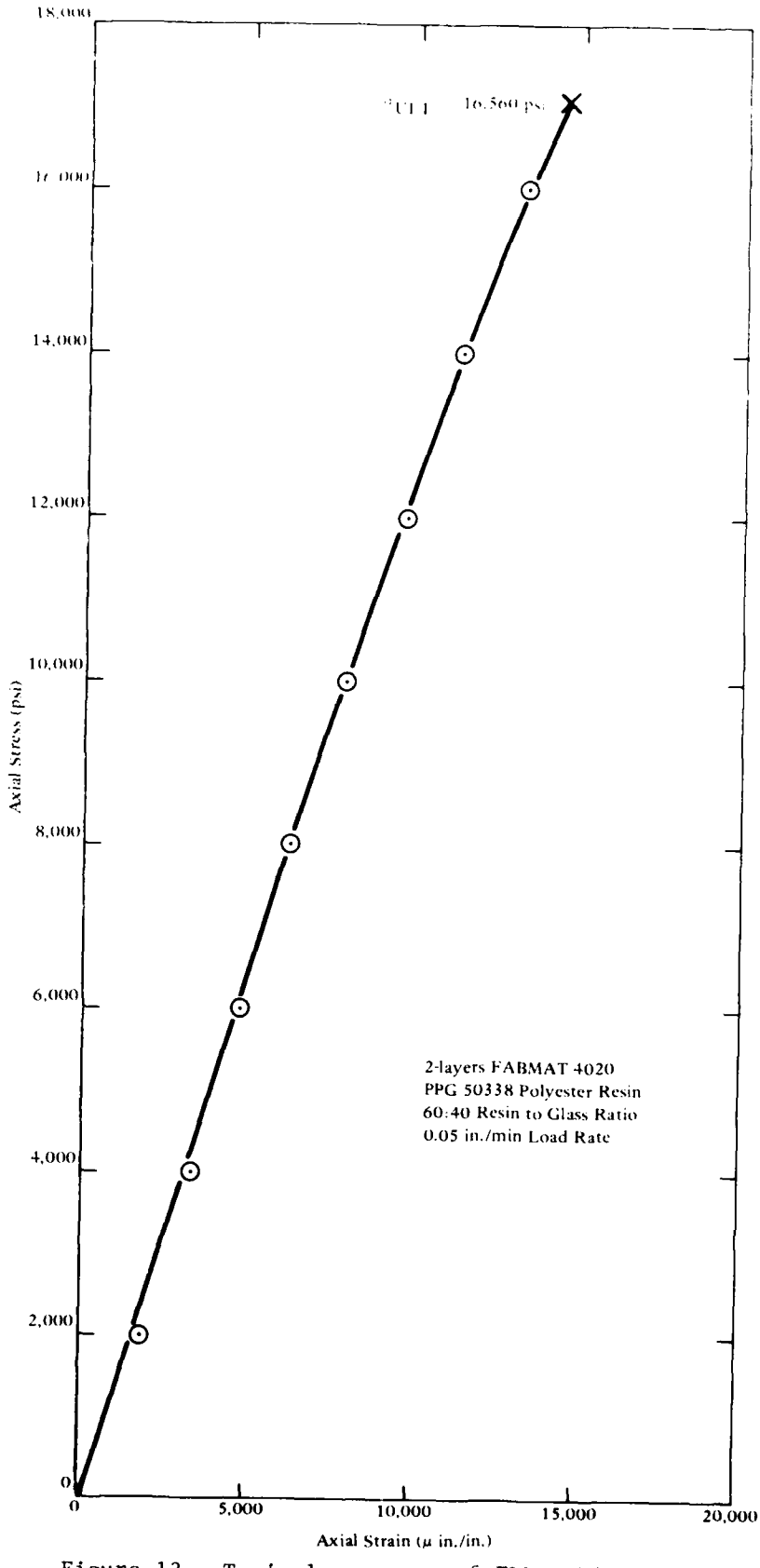

Figure 13. Typical response of FRP subjected to uniaxial tension parallel to roving.

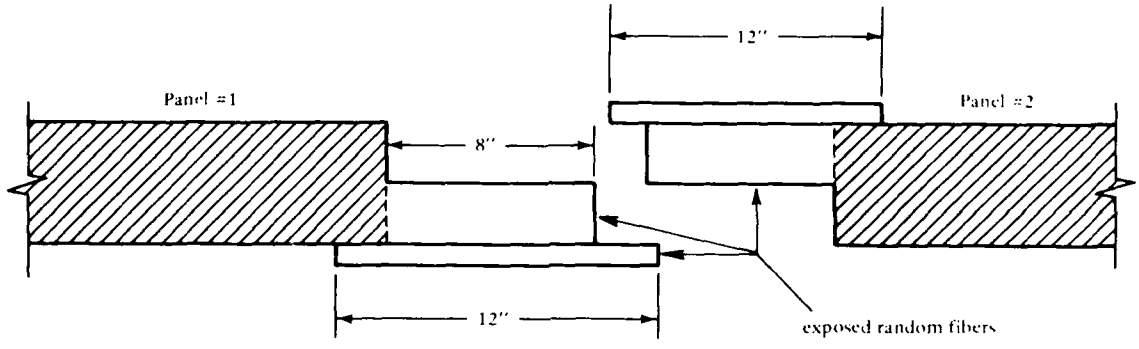

Basic Panel Thickness: 4 plies
Lap Thickness: 2 plies
Splice Plates:
Top – 1 ply
Bottom – 1 ply

Field Saturated
Prefabricated

Construction Method: Set bottom (unsaturated) splice plate in position. Place panel #1 as shown. Position panel #2 with edges overlapping edges of panel #1. Fold back edges of panel #2 and apply polyester resin to edges of panel #1. Re-position edges of panel #2 and saturate with polyester resin. Position upper splice plate and saturate with resin. Roll edges to expel trapped air. The bottom splice plate will be saturated by resin draining through the lapped edges.

Materials: 4020 fiberglass
PPG Industries RS 50338 polyester resin

Figure 14. Panel joining method A.

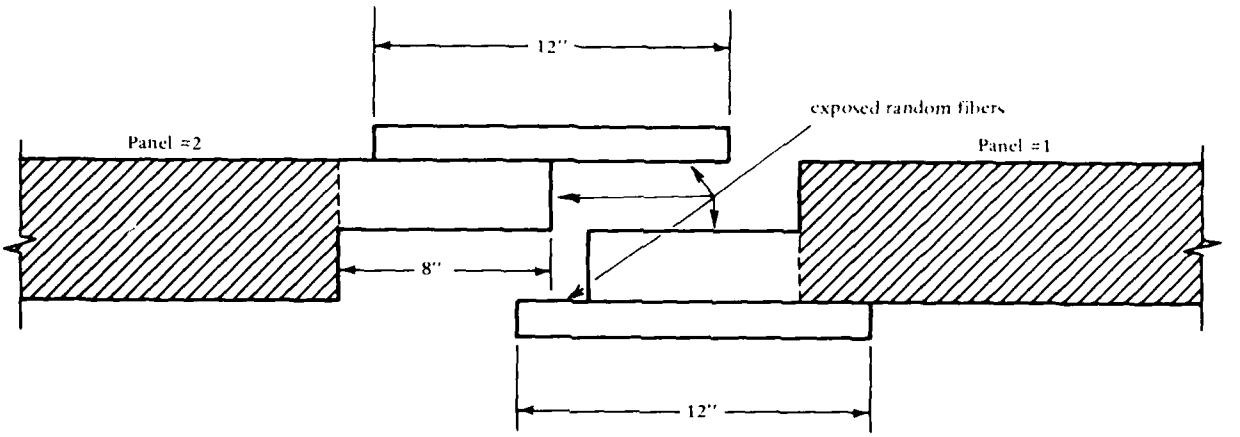

Basic Panel Thickness: 4 plies
Lap Thickness: 2 plies
Splice Plates:
Top - 1 ply
Bottom - 1 ply

Field Saturated
Prefabricated

Construction Method: Set bottom (unsaturated) splice plate in position. Place panel #1 as shown. Position panel #2 with edges overlapping edges of panel #1. Fold back edges of panel #2 and apply polyester resin to edges of panel #1. Re-position edges of panel #2 and saturate with resin. Position upper splice plate and saturate with resin. Roll edges to expel trapped air. The bottom splice plate will be saturated by resin draining through the lapped edges.

Materials: 4020 fiberglass
PPG Industries RS 50338 polyester resin

Figure 15. Panel joining method B.

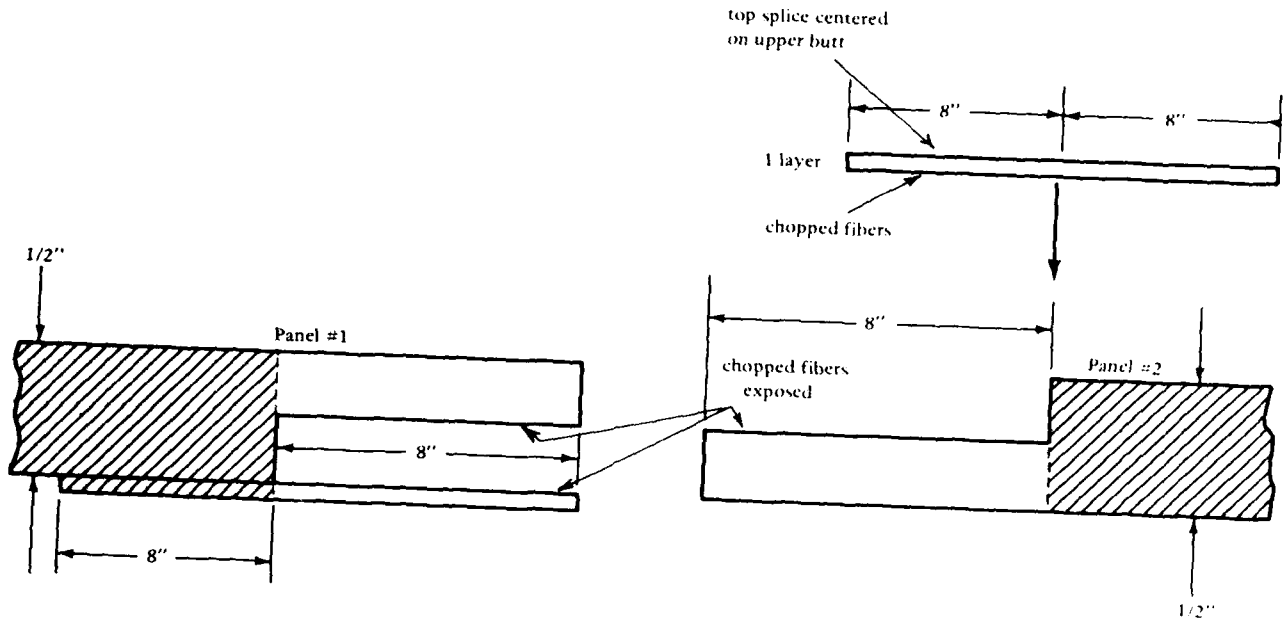

Basic Panel Thickness: 4 plies
Lap Thickness: 2 plies
Splice Plates:
Top - 1 ply
Bottom - 1 ply

Field Saturated
Prefabricated

Construction Method: One half of bottom splice plate prefabricated with panel #1. Remaining half of splice plate would be of unsaturated fiberglass. Position panel #1 and fold back top edges. Place panel #2 with edges over bottom splice plate and butting against panel #1. Saturate edges of panel #2 and bottom splice plate with polyester resin. Release edges of panel #1 and saturate with resin. Center top splice plate on top butt of joint and saturate with resin. Roll joint to expel trapped air.

Materials: 4020 fiberglass
PPG Industries RS 50338 polyester resin

Figure 16. Panel joining method C.

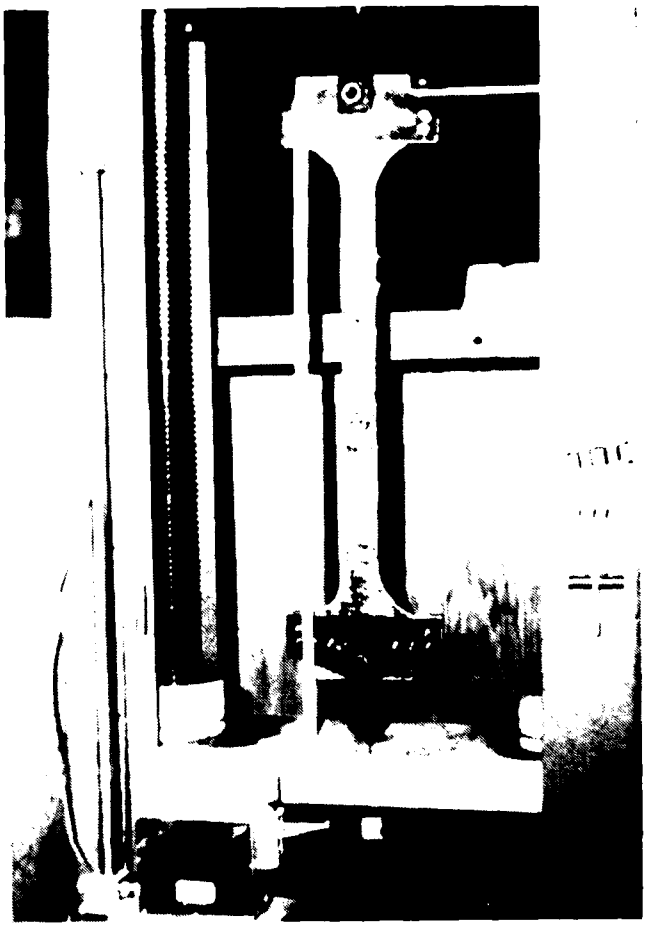

Figure 17. Tensile test of panel joints.

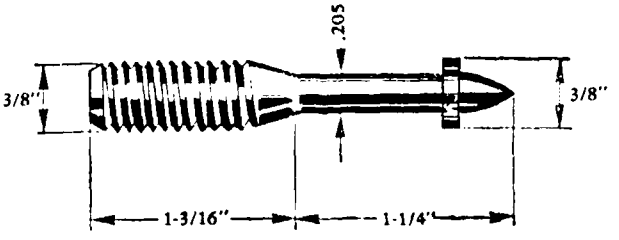

Figure 18. Hilti fastener number W10-30-32 P10.

Figure 19. FRP panel for tiedown testing.

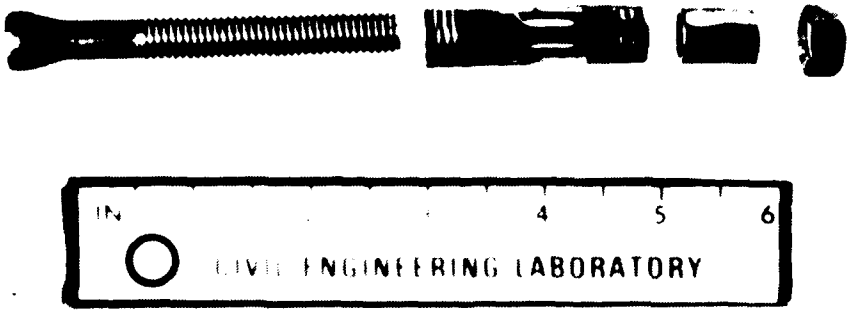

Figure 20. Torque-set fastener, 1/2-in. x 3-in.

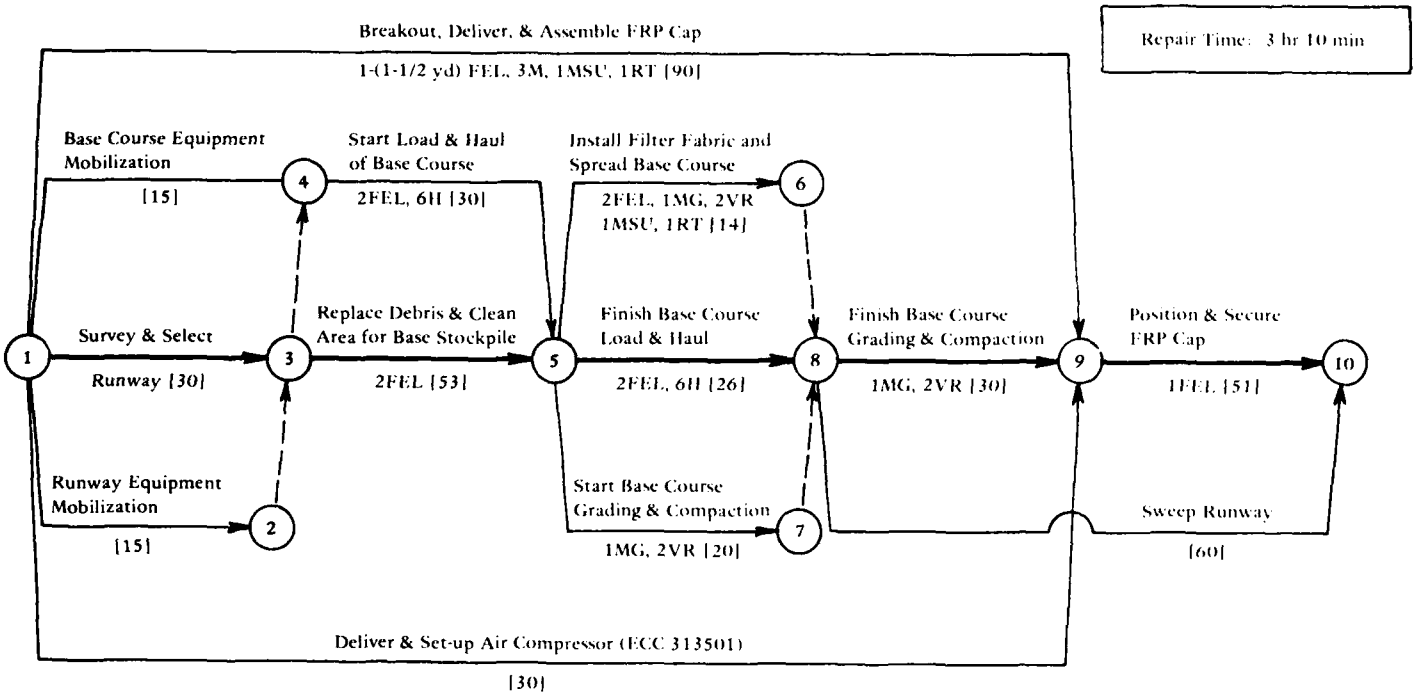

Note:

1. Duration estimates for activities 1-3, 5-7, 8-9 and 8-10 from Reference 13.
2. ○——→○ Denotes critical path.
3. [30] Denotes repair time in minutes.
4. Total repair time equals the summation of repair times for critical path activities.

Equipment Needed and Abbreviations

FEL	Front End Loader, 5-1/2 yd^3, ECC 453151
H	Hauler, 30T, ECC 480501
VR	Vibratory Roller, ECC 463521
MG	Motor Grader, ECC 442031
M	Miscellaneous, 7,000 lb drawbar pull
MSU	Manual Spray Unit (Polyester Resin)
RT	Rough Terrain Forklift, ECC 130400
ECC	Equipment Classification Code

Figure 21. Flow network for repair of a single 750-lb bomb crater.

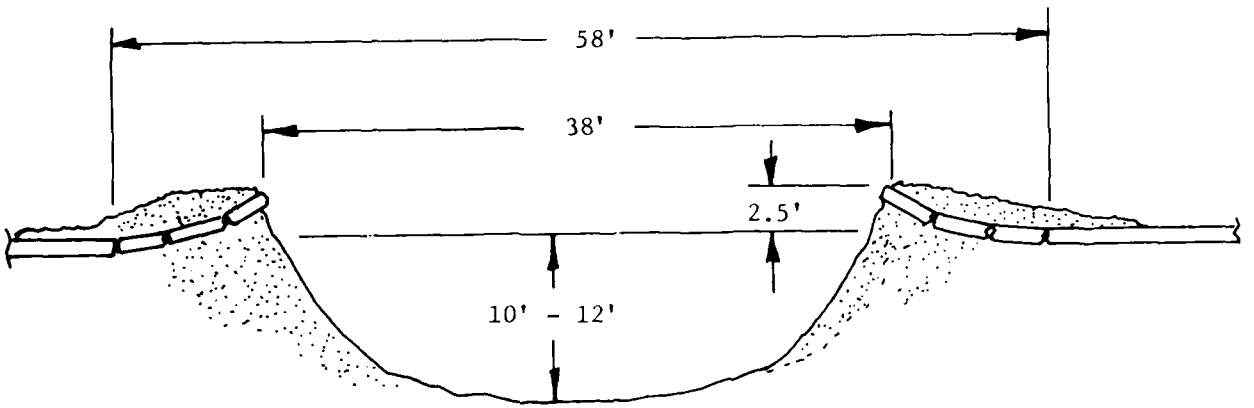

Ejecta: 260 cu yd
Upheaval Removal: 56 cu yd

Figure 22. Typical 750-lb bomb crater (Ref 14).

Appendix A

RRR TEST FACILITY*

A permanent facility was constructed at Tyndall AFB, Fla. by the Air Force Civil Engineering Center, Directorate of Field Technology, to allow accelerated traffic tests of various pavement repair materials and designs. A clay core 60 feet wide, 220 feet long and 6 feet deep was placed and compacted at a high water content to provide a weak test subgrade. Twelve inches of crushed limestone was placed as a base course followed by a 10-inch-thick portland cement concrete pavement. Three 20- by 20-ft sections were left open in the concrete to serve as test pits. The local dune sand was stabilized with oyster shells to construct a sand fill around the test site. The local water table fluctuates and during wet seasons is at approximately the surface of the natural sand subgrade.

The 20-foot test pits provide a location to construct representative pavement repairs. The depth to the clay subgrade can be varied by adding or removing clay as necessary. Following traffic on any test repair, the repair materials can be removed, and a different repair constructed in the same pit.

The test pits do not try to duplicate the crater repair problem. Because of the many variations in crater types and sizes and their very erratic geometry (Ref 16), attempts to construct model representative craters would be futile. Instead, the dimensions of the test pits were selected to provide a controlled test of the joint between the pavement and the repair and also, in the middle of the test pit, to test the repair performance over a soft subgrade with a minimum effect from edge conditions. The 20-foot dimension is also considered as the approximate point where use of a landing mat patch becomes less desirable and though airfield pavement slab sizes vary tremendously, it is felt to be representative of airfield slab sizes.

Portable covers were constructed to protect the test pits from rain, but it was necessary to supplement these with rubber seals glued into shallow saw cuts approximately 6 inches from the edge of the test pit. A "snow fence" was also erected around the test pad to reduce problems with blowing and drifting sand. A prefabricated building is presently being erected over the site to allow testing during inclement weather.

*Reprinted from Reference 15.

The clay used for the test subgrade is a local clay obtained from near Wewahitchka, Fla. It is classified as CH under the Unified Soil Classification System (Ref 17). Table A-1 shows physical properties and Table A-2 mineralogical composition of the clay. This clay was placed at an average moisture content of 27% and a California Bearing Ratio (CBR) of 4. This strength was selected as a representative lower bound for crater debris backfill based on eight previous crater repair field tests (Ref 18).

Each repair was subjected to simulated F-4 traffic. The load cart applies a 27,000-pound gear load at a 265-psi tire pressure. Traffic is applied in an approximately normal distribution over a 10-foot traffic lane. The load cart is pulled forward and then backed up in the same wheel path. Consequently, a total of 96 passes of the load are placed on the test item to obtain 10 coverages of the traffic in the center lane with 8 coverages in the adjacent lanes and 2 coverages in the outside lanes. A normal distribution is representative of actual aircraft traffic distribution on a runway and avoids introducing a sharp discontinuity between trafficked and untrafficked areas (Ref 19).

Table A-1. Physical Properties of Wewahitchka Clay

Property	Range	Average
Liquid Limit	57 - 79	65
Plastic Limit	21 - 30	25
Plasticity Index	30 - 52	40
Specific Gravity	2.580 - 2.67	2.61
CE-55 Dry Density[a]	110 - 115 pcf	113 pcf
Moisture[a]	13 - 15%	14.5%
CE-26 Dry Density[a]	105 - 109 pcf	107 pcf
Moisture[a]	13 - 16.5%	14.5%
CE-12 Dry Density[a]	98 - 102.5 pcf	99.0 pcf
Moisture[a]	11.5 - 18%	15.0%

[a]Optimum.

Table A-2. Mineralogical Composition of Wewahitchka Clay

Mineral Constituents	Relative Sample Content*
Clay	
Kaolinite	Intermediate
Smectite	Common
Clay-mica	Common
Non Clays	
Quartz	Intermediate
Feldspars	Rare

*Based on the following:

Abundant	> 50%
Intermediate	25 - 50%
Common	10 - 25%
Minor	5 - 10%
Rare	> 5%

Appendix B

SOIL TESTING AND ANALYSIS

Samples of the heavy clay soil (Wewahitchka Clay) and crushed limestone base course (Tyndall Crushed Stone) used in RRR testing at Tyndall AFB, Fla., were obtained from the AFESC/RDCR. The clay was received at a moisture content of 42% (by weight) and allowed to air dry until moisture content had lowered to approximately 28%. The sample was then thoroughly mixed to insure uniformity and placed in a sealed container to prevent moisture loss. Samples were prepared for triaxial shear testing using a 2.8-in.-diam mold. Samples were compacted by hand-tamping into the mold in five equal layers. The soil for each layer was weighed and layer height controlled to give a compacted density equal to a pre-determined density which corresponded to that of the clay in the Tyndall subgrade. Nominal clay density, water content, and sample height were 95 pcf (dry density), 28% by weight, and 6 inches, respectively.

In consideration of the rapid nature of the loading which would be produced by the moving wheel load of the test cart and the impermeability of the clay, unconsolidated-undrained triaxial tests were conducted. Samples were prepared and tested at a moisture content corresponding to that of the Tyndall subgrade, and thus were not in a completely saturated condition at start of the triaxial tests. The test apparatus was a CKC e/p cyclic loader developed by Dr. Clarence Chan, research engineer and lecturer of the University of California at Berkeley. Each sample was subjected to a confining pressure and, with cell drainage lines closed, immediately (2 to 4 minutes) loaded at a rate of approximately 5 psi/min. Samples were tested to failure at three different confining pressures. Plots of soil response are presented in Figure B-1, and the Mohr failure envelopes are depicted in Figure B-2. The shearing strength of the clay is represented by the cohesion since the test circumstances resulted in the $\phi = 0$ condition.*

*The pore pressure of a saturated cohesive sample triaxial tested in an undrained condition acts with equal intensity in all directions; thus, the increment of pore pressure is the same for both major and minor principal stresses. The failure circle for each test has the same diameter whether it is plotted in terms of effective stresses or total stresses. If several samples are tested under undrained conditions at different cell pressures, the rupture line with respect to total stresses (Figure B-2) is horizontal.

Although not completely saturated, the tested samples of Wewahitchka clay were compacted at above optimum moisture content (27% vs. 17%) with a degree of saturation of 94%. This high degree of saturation led to performance of the clay as, essentially, a saturated sample. Previous research conducted on not fully saturated clays compacted at above optimum moisture content has indicated a horizontal failure envelope for triaxial tests conducted on samples in an undrained condition and at confining pressures up to 1,000 psi (Ref 20).

The Tyndall crushed stone underwent a mechanical sieve analysis (Figure B-3), and a moisture-density relations test (Figure B-4) was conducted to specifications of ASTM Test Designation D698-70, Method C (Ref 12). The maximum grain size was 1-1/2 inches, and the maximum dry density was 141 pcf at 6% moisture content.

Apparatus was not readily available for triaxial testing of samples having diameters greater than 2.8 inches. Diameters of triaxial samples consisting of well-graded materials should exceed the maximum grain size by at least six times (Ref 21). Accordingly, the soil for triaxial samples was split on the 3/4-inch and no. 4 sieves and the material retained on the 3/4-inch sieve was replaced by an equivalent weight of material passing the 3/4-inch and retained on the no. 4 sieve; thus, approximately 20% of the sample grain size distribution was altered. The resulting material mixture had maximum particle sizes of approximately 1/2 inch, thereby marginally passing the criteria for molding into 2.8-in.-diam triaxial test specimens.

The change in grain size distribution will have some effect on sample behavior. Research reported in Reference 22 has found the following change in parameters resulting from a reduction in maximum particle size:

- Axial Strain at Failure - lower
- Angle of Internal Friction - greater
- Initial Tangent Modulus - greater

This evidence would suggest an under-conservative prediction of soil strength.

Samples were prepared in a 2.8-in.-diam mold by compaction, using a surcharge of 11 pounds and a vibrator with a frequency of 3,500 cpm. Samples were compacted in five equal layers; and material weight, moisture content, and layer height were pre-calculated to give the required finished density of the sample. Sample density was re-checked after molding. Nominal sample moisture content, dry density, and height were 5%, 140 pcf, and 6 inches, respectively.

The Tyndall crushed stone was tested in a consolidated-drained condition as a result of its permeability - rapid draining - characteristics. Samples were tested with sample drain lines open and at confining pressures of 10 and 15 psi. A stress-controlled rate of approximately 14 psi/min was used. The samples were consolidated for 5 minutes prior to application of deviator stress. Material response to load (Figure B-5) and Mohr failure envelope (Figure B-6) were plotted.

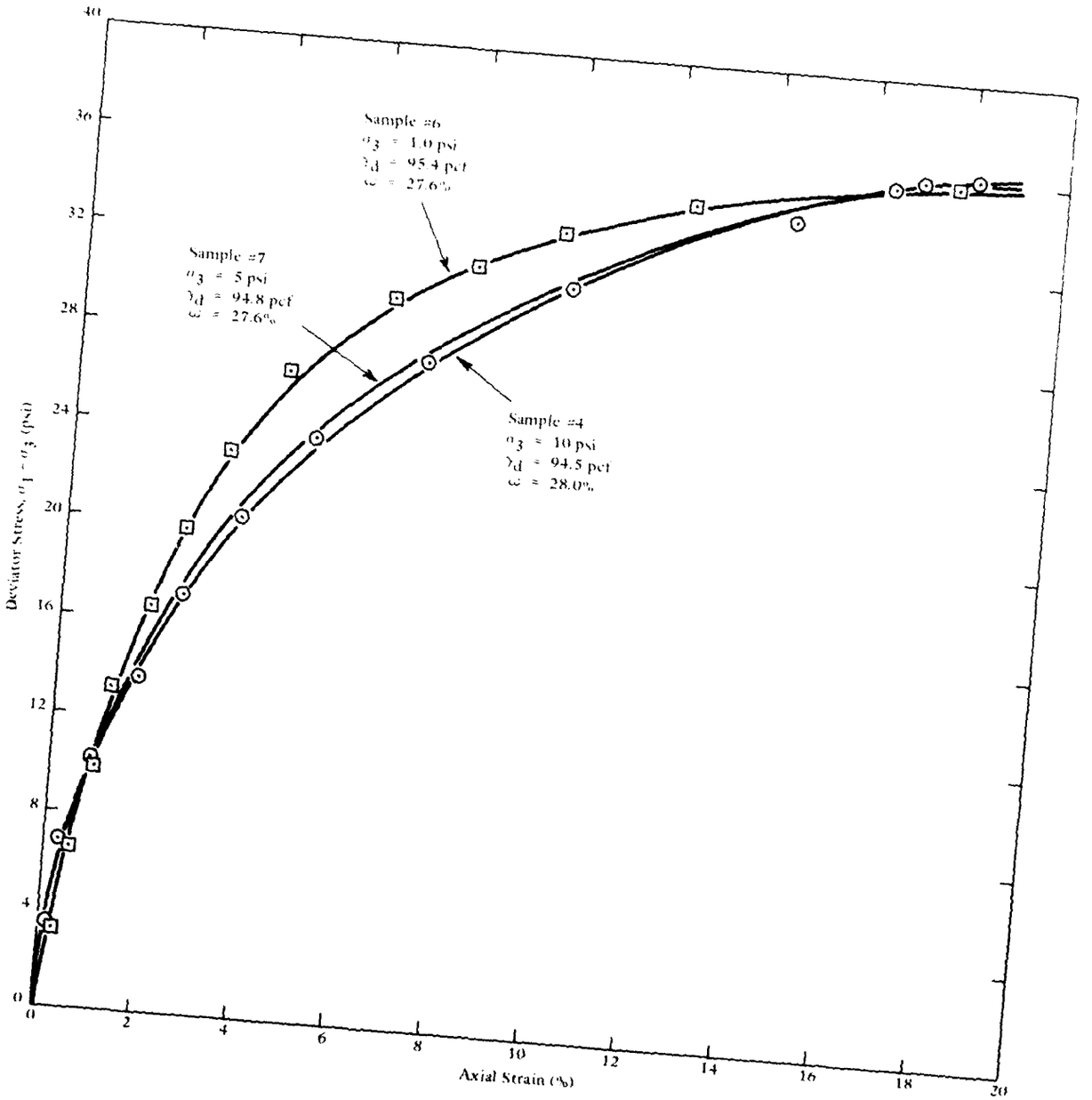

Figure B-1. Response characteristics of Wewahitchka clay triaxial tested in an unconsolidated-undrained condition.

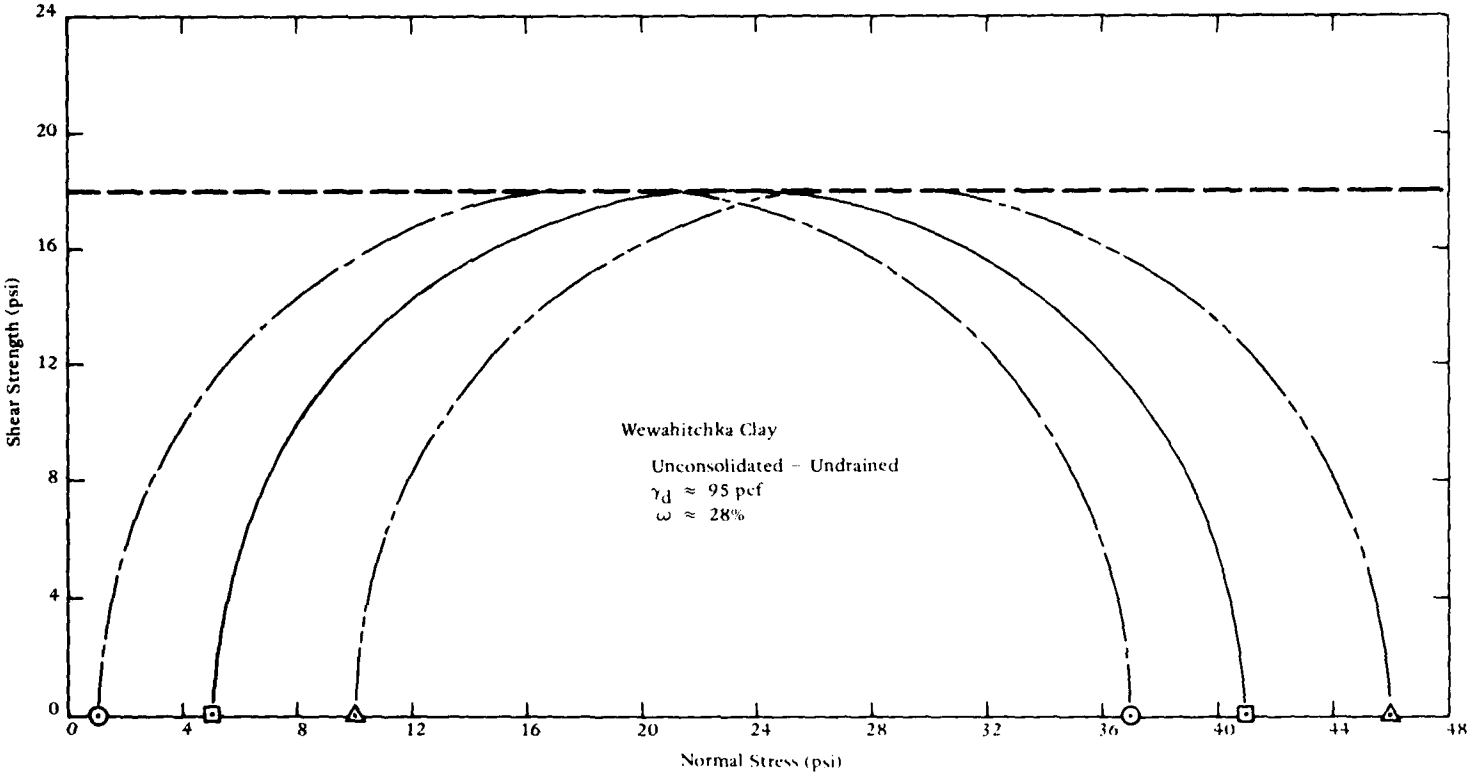

Figure B-2. Failure envelopes for Wewahitchka clay triaxial tested in an unconsolidated-undrained condition.

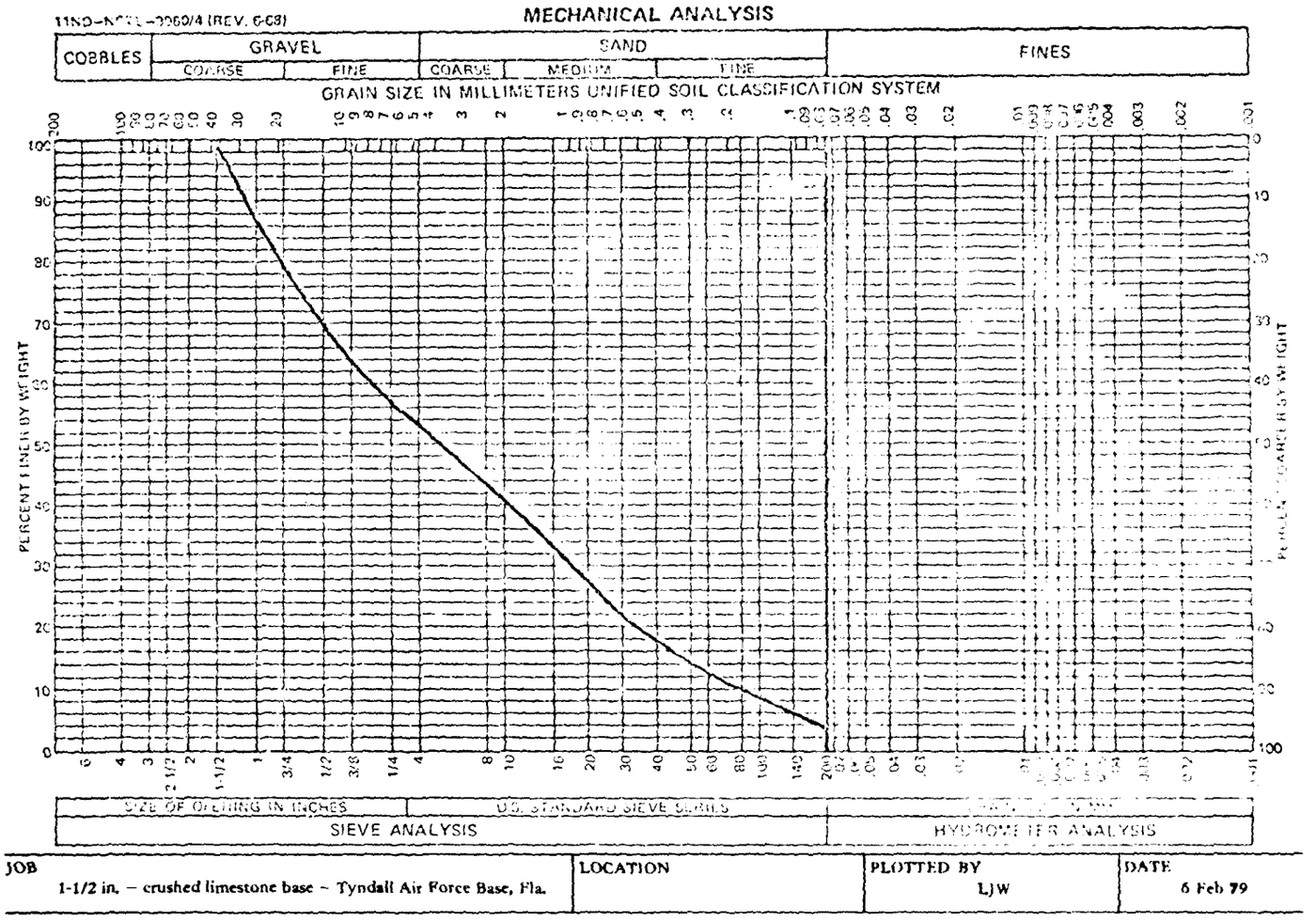

Figure B-3. Grain size distribution of Tyndall crushed stone.

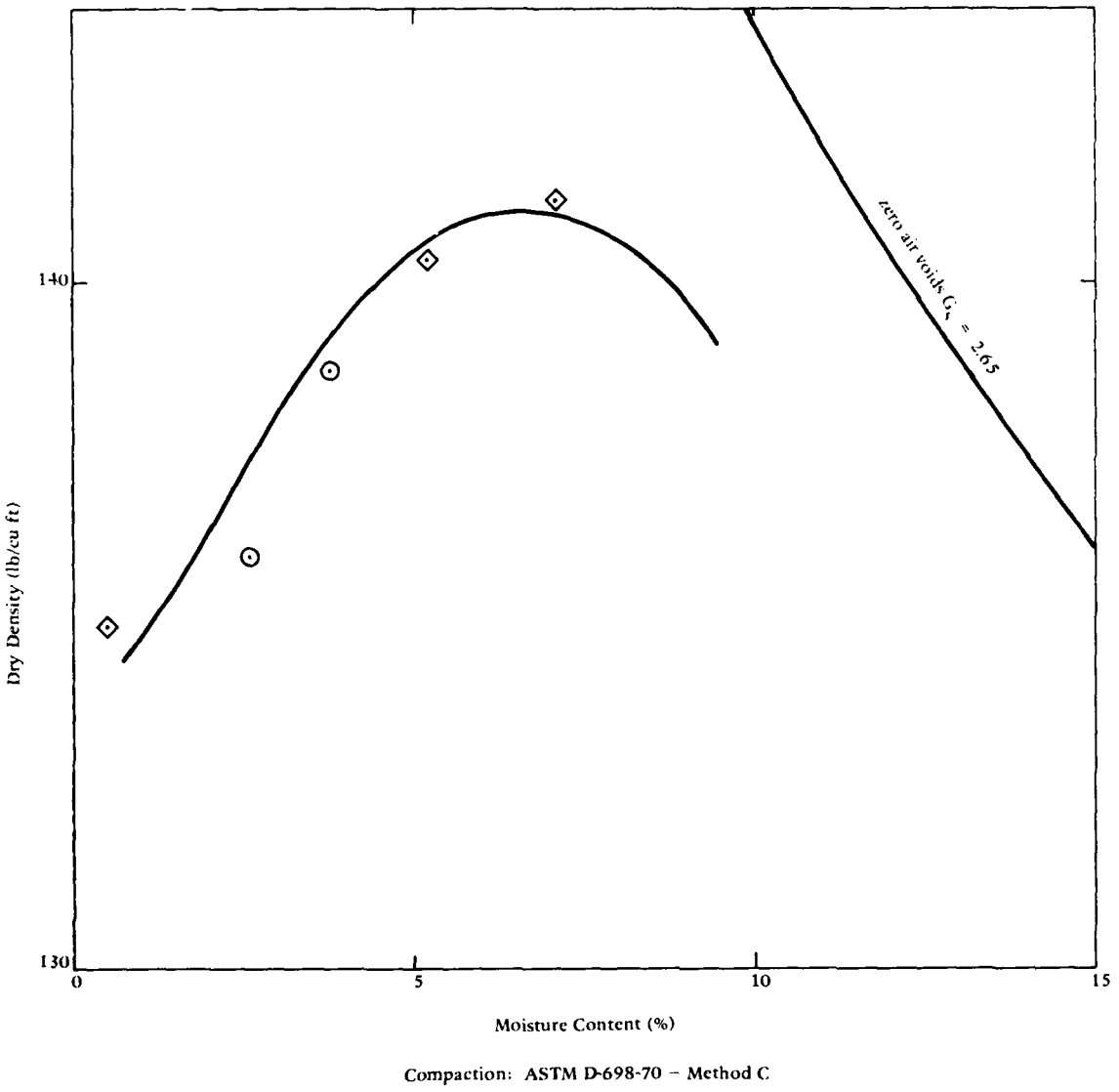

Figure B-4. Moisture-density relations for Tyndall crushed stone.

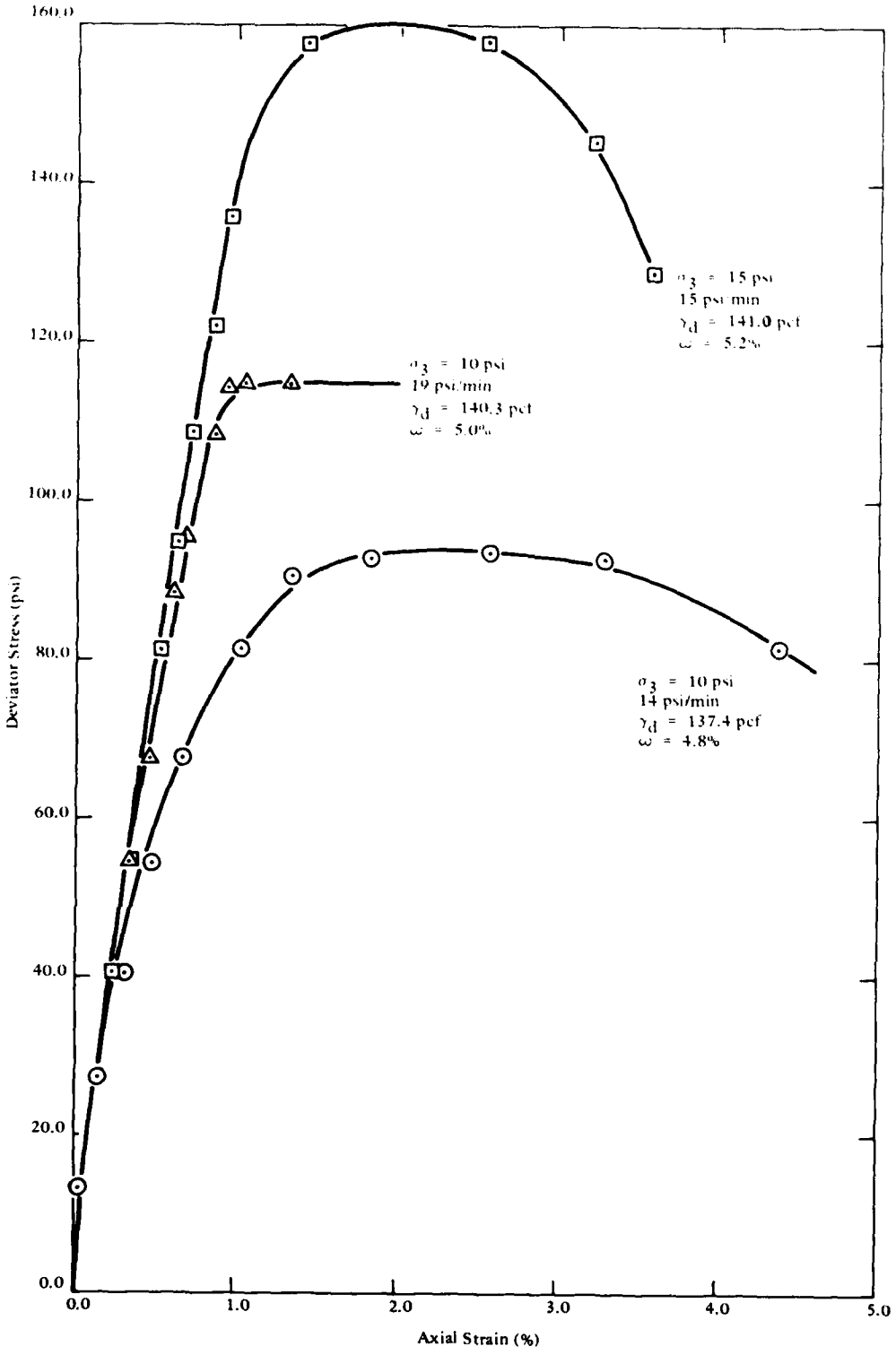

Figure B-5. Response characteristics of Tyndall crushed stone triaxial tested in a consolidated-drained condition.

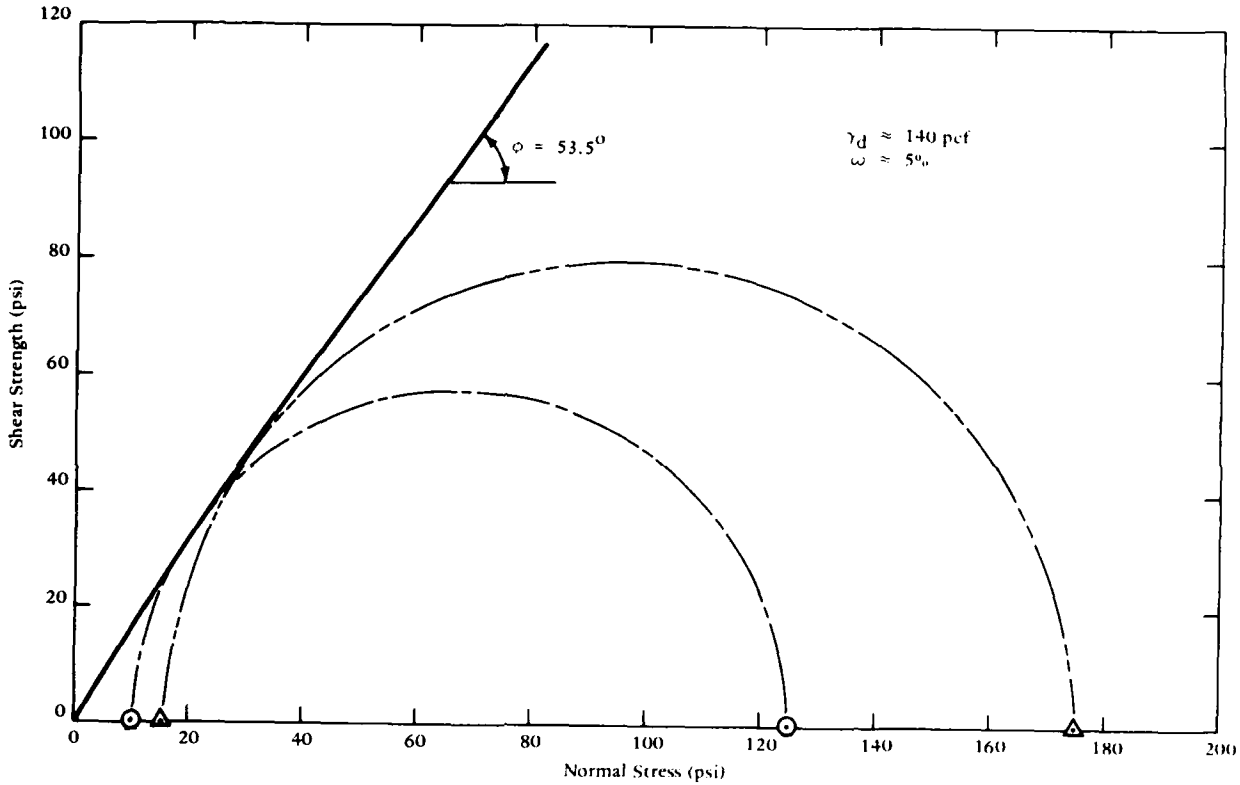

Figure B-6. Failure envelope for Tyndall crushed stone triaxial tested in a consolidated-drained condition.

DISTRIBUTION LIST

AFB (AFIT LD), Wright-Patterson OH; AF Tech Office (Mgt & Ops), Tyndall, FL; CESCH, Wright-Patterson; HQ Tactical Air Cmd (R. E. Fisher), Langley AFB VA; HQAFESC DEMM, Tyndall AFB, FL; MAC DEE (Col. P. Thompson) Scott, IL; Stinfo Library, Offutt NE
ARMY BMDSC-RE (H. McClellan) Huntsville AL; DAEN-MPE-D Washington DC; HQ-DAEN-MPO-B (Mr. Price)
ARMY - CERL Library, Champaign IL
ARMY COE Philadelphia Dist. (LIBRARY) Philadelphia, PA
ARMY CORPS OF ENGINEERS MRD-Eng. Div., Omaha NE; Seattle Dist. Library, Seattle WA
ARMY CRREL R.A. Eaton
ARMY DARCOM AMCPM-CS (J. Carr), Alexandria VA
ARMY ENG WATERWAYS EXP STA Library, Vicksburg MS
ARMY ENVIRON. HYGIENE AGCY Water Qual Div (Doner), Aberdeen Prov Ground, MD
ARMY MATERIALS & MECHANICS RESEARCH CENTER Dr. Lenoe, Watertown MA
ARMY TRANSPORTATION SCHOOL MAJ T Sweeney, Code ATSP CD-TE Fort Eustis VA
ASST SECRETARY OF THE NAVY Spec. Assist Energy (Leonard), Washington, DC
CINCLANT Civil Engr. Supp. Plans. Ofr Norfolk, VA
CINCPAC Fac Engrng Div (J44) Makalapa, HI
CNM NMAT 08T246 (Dieterle) Wash, DC
CNO Code NOP-964, Washington DC
COMCBPAC Operations Off, Makalapa HI
COMFAIRWESTPAC Security Offr, Misawa Japan
COMNAVBEACHPHIBREFTRAGRU ONE San Diego CA
COMNAVMARIANAS Code N4, Guam
COMOCEANSYSPAC SCE, Pearl Harbor HI
COMSUBDEVGRUONE Operations Offr, San Diego, CA
DEFENSE DOCUMENTATION CTR Alexandria, VA
DLSIE Army Logistics Mgt Center, Fort Lee, VA
DNA STTL, Washington DC
FMFLANT CEC Offr, Norfolk VA
MARINE CORPS BASE Code 43-260, Camp Lejeune NC; M & R Division, Camp Lejeune NC; PWO Camp Lejeune NC; PWO, Camp S. D. Butler, Kawasaki Japan
MARINE CORPS HQS Code LFF-2, Washington DC
MCAS Facil. Engr. Div. Cherry Point NC; Code PWE, Kaneohe Bay HI; Code S4, Quantico VA; PWO Kaneohe Bay HI; PWO, Yuma AZ; SCE, Futema Japan
MCDEC NSAP REP, Quantico VA; P&S Div Quantico VA
MCLSBPAC PWO, Barstow CA
NAF PWD - Engr Div, Atsugi, Japan; PWO Sigonella Sicily; PWO, Atsugi Japan
NAS CO, Guantanamo Bay Cuba; Code 114, Alameda CA; Code 183 (Fac. Plan BR MGR); Code 18700, Brunswick ME; Code 18U (ENS P.J. Hickey), Corpus Christi TX; Code 70, Atlanta, Marietta GA; Dir. Maint. Control Div., Key West FL; Dir. Util. Div., Bermuda; ENS Buchholz, Pensacola, FL; Lakehurst, NJ; PW (J. Maguire), Corpus Christi TX; PWD Maint. Cont. Dir., Fallon NV; PWD Maint. Div., New Orleans, Belle Chasse LA; PWD, Maintenance Control Dir., Bermuda; PWD, Willow Grove PA; PWO Belle Chasse, LA; PWO Chase Field Beeville, TX; PWO Key West FL; PWO Whiting Fld, Milton FL; PWO, Dallas TX; PWO, Glenview IL; PWO, Kingsville TX; PWO, Millington TN; PWO, Miramar, San Diego CA; PWO,, Moffett Field CA; ROICC Key West FL; SCF Lant Fleet Norfolk, VA; SCE Norfolk, VA; SCE, Barbers Point HI
NATL RESEARCH COUNCIL Naval Studies Board, Washington DC
NATPARACHUTETESTRAN PW Engr, El Centro CA
NAVACT PWO, London UK
NAVAEROSPREGMEDCEN SCE, Pensacola FL
NAVCOASTSYSCEN Code 772 (C B Koesy) Panama City FL
NAVCOASTSYSTCTR Code 713 (J. Quirk) Panama City, FL; Library Panama City, FL
NAVCOMMAREAMSTRSTA PWO, Norfolk VA; PWO, Wahiawa HI; SCE Unit 1 Naples Italy
NAVCOMMSTA Code 401 Nea Makri, Greece; PWO, Exmouth, Australia
NAVEDTRAPRODEVCEN Tech. Library
NAVEDUTRACEN Engr Dept (Code 42) Newport, RI
NAVFAC PWO, Centerville Bch, Ferndale CA

NAVFAC PWO, Lewes DE
NAVFACENGCOM Code 043 Alexandria, VA; Code 044 Alexandria, VA; Code 0451 Alexandria, VA; Code 04543B Alexandria, Va; Code 04B5 Alexandria, VA; Code 100 Alexandria, VA; Code 1002B (J. Lehmann) Alexandria, VA; Code 1113 (L. Stevens) Alexandria, VA; Morrison Yap, Caroline Is.; P.W. Brewer Alexandria, VA
NAVFACENGCOM - CHES DIV, Code 101 Wash, DC; Code 102, (Wildman), Wash, DC; Code 405 Wash, DC
NAVFACENGCOM - LANT DIV, Code 405, Norfolk, VA; Fac. BR Deputy Dir, Naples Italy, European Branch, New York; RDT&E O 102, Norfolk VA
NAVFACENGCOM - NORTH DIV, CO; Code 09P (LCDR A.J. Stewart); Code 102; Code 1028; RDT&E O, Philadelphia PA
NAVFACENGCOM - PAC DIV, (Kyl) Code 101, Pearl Harbor, HI; Code 2011 Pearl Harbor, HI; Code 402, RDT&E, Pearl Harbor HI; Commander, Pearl Harbor, HI
NAVFACENGCOM - SOUTH DIV, Code 405, RDT&E O, Charleston, SC; Code 90, RDT&E O, Charleston SC
NAVFACENGCOM - WEST DIV, 102; Code 04B San Bruno, CA; 09P 20 San Bruno, CA; RDT&E O Code 2011 San Bruno, CA
NAVFACENGCOM CONTRACT AROICC, Point Mugu CA; Eng Div dir, Southwest Pac, Manila, PI; OIC C, Southwest Pac, Manila, PI; OICC/ROICC, Balboa Canal Zone; ROICC AF Guam; ROICC LANT DIV, Norfolk VA; ROICC Off Point Mugu, CA; ROICC, Keflavik, Iceland
NAVHOSP L I R, Elsbernd, Puerto Rico
NAVPETOFF Code 30, Alexandria VA
NAVPHIBASE CO, ACB 2 Norfolk, VA; Code S3L, Norfolk VA
NAVREGMEDCEN SCE (D. Kaye); SCE, Camp Pendleton CA
NAVSCOLCECOFF C35 Port Hueneme, CA
NAVSEASYSCOM Code 0325, Program Mgr, Washington, DC
NAVSECGRUACT PWO, Adak AK
NAVSHIPYD Code 404 (LT J. Riccio), Norfolk, Portsmouth VA; Code 410, Mare Is., Vallejo CA; Code 440 Portsmouth NH; Code 440, Puget Sound, Bremerton WA; Tech Library, Vallejo, CA
NAVSTA CO Roosevelt Roads P.R. Puerto Rico; Maint. Div. Dir Code 531, Rodman Canal Zone; PWD (LTJG P.M. Motolenich), Puerto Rico; PWO, Guantanamo Bay Cuba; PWO, Keflavik Iceland; PWO, Mayport FL; SCE, San Diego CA; SCE, Subic Bay, R.P.
NAVSUPPACT LTJG McGarrah, SEC, Vallejo, CA
NAVSURFWPNCEN PWO, White Oak, Silver Spring, MD
NAVTECHTRACEN SCE, Pensacola FL
NAVWPNCEN Code 2636 (W. Bonner), China Lake CA
NAVWPNSTA PW Office (Code 09C1) Yorktown, VA
NAVWPNSTA PWO, Seal Beach CA
NAVWPNSUPPCEN Code 09 Crane IN
NCBC 405 OIC, San Diego, CA
NCBC CEL AOIC Port Hueneme CA; Code 10 Davisville, RI; Code 155, Port Hueneme CA; Code 156, Port Hueneme, CA; Code 400, Gulfport MS; PWO, Davisville RI
NCR 20, Commander
NMCB 5, Operations Dept.; 74, CO; Forty, CO; THREE, Operations Off.
NORDA Code 440 (Ocean Rsch Off) Bay St. Louis MS
NSD SCE, Subic Bay, R.P.
NTC OICC, CBU-401, Great Lakes IL
NUSC Code 131 New London, CT; Code EA123 (R.S. Munn), New London CT
ONR Code 700F Arlington VA; Dr. A. Laufer, Pasadena CA
PACMISRANFAC CO, Kekaha HI
PHIBCB 1 P&E, Coronado, CA
PMTC Pat. Counsel, Point Mugu CA
PWC CO Norfolk, VA; CO, Great Lakes IL; CO, Oakland CA; Code 120, Oakland CA; Code 120C, (Library) San Diego, CA; Code 128, Guam; Code 200, Guam; Code 220 Oakland, CA; Code 220.1, Norfolk VA; Code 30C, San Diego, CA; Code 400, Pearl Harbor, HI; Code 400, San Diego, CA; Code 610, San Diego Ca; Library, Subic Bay, R.P.; Utilities Officer, Guam; XO Oakland, CA
MARCORPS 1st Marine Div (LT Galvez), Camp Pendleton, CA
U.S. MERCHANT MARINE ACADEMY Kings Point, NY (Reprint Custodian)
US NAVAL FORCES Korea (ENJ-P&O)
USCG G-EOE-4/61 (T. Dowd), Washington DC
USDA Forest Service, Bowers, Atlanta, GA; Forest Service, San Dimas, CA

USEC COMLECH-LEO, Wright, Stuttgart, GI
FLORIDA ATLANTIC UNIVERSITY Boca Raton FL (Ocean Engr Dept., C. Lin)
IOWA STATE UNIVERSITY Ames IA (CE Dept, Handy)
LEHIGH UNIVERSITY Bethlehem PA (Fritz Engr. Lab No. 13, Beedle); Bethlehem PA (Linderman Lib. No. 30, Hecksteiner)
LIBRARY OF CONGRESS WASHINGTON, DC (SCIENCES & TECH DIV)
MICHIGAN TECHNOLOGICAL UNIVERSITY Houghton, MI (Haas)
MIT Cambridge MA; Cambridge MA (Rm 10-500, Tech. Reports, Engr. Lib.)
OREGON STATE UNIVERSITY CORVALLIS, OR (CE DEPT, BELL); CORVALLIS, OR (CE DEPT, HICKS)
PURDUE UNIVERSITY Lafayette IN (Leonards); Lafayette, IN (Altschaeffl); Lafayette, IN (CE Engr. Lib)
TEXAS A&M UNIVERSITY W.B. Ledbetter College Station, TX
UNIVERSITY OF CALIFORNIA BERKELEY, CA (CE DEPT, MITCHELL)
UNIVERSITY OF ILLINOIS Metz Ref Rm, Urbana IL; URBANA, IL (LIBRARY)
UNIVERSITY OF MASSACHUSETTS (Heronemus), Amherst MA CE Dept
UNIVERSITY OF NEBRASKA-LINCOLN Lincoln, NE (Ross Ice Shelf Proj.)
UNIVERSITY OF NEW MEXICO J Nielson-Engr Matls & Civil Sys Div, Albuquerque NM
UNIVERSITY OF WASHINGTON Seattle, WA Transportation, Construction & Geom. Div
AMETEK Offshore Res. & Engr Div
ARVID GRANT OLYMPIA, WA
ATLANTIC RICHFIELD CO. DALLAS, TX (SMITH)
AUSTRALIA Dept. PW (A. Hicks), Melbourne
BECHTEL CORP. SAN FRANCISCO, CA (PHELPS)
BROWN & CALDWELL E. M Saunders Walnut Creek, CA
CANADA Mem Univ Newfoundland (Chari), St Johns; Surveyor, Nenninger & Chenevert Inc., Montreal; Trans-Mnt Oil Pipe Line Corp. Vancouver, BC Canada
GLIDDEN CO. STRONGSVILLE, OH (RSCH LIB)
HALEY & ALDRICH, INC. Cambridge MA (Aldrich, Jr.)
MC CLELLAND ENGINEERS INC Houston TX (B. McClelland)
MCDONNEL AIRCRAFT CO. Dept 501 (R.H. Fayman), St Louis MO
NORWAY J. Creed, Ski
PORTLAND CEMENT ASSOC. SKOKIE, IL (CORLEY); Skokie IL (Rsch & Dev Lab, Lib.)
RAYMOND INTERNATIONAL INC. F Colle Soil Tech Dept, Pennsauken, NJ
TIDEWATER CONSTR. CO Norfolk VA (Fowler)
UNITED KINGDOM Cement & Concrete Assoc Wexham Springs, Slough Bucks; D. Lee, London; D. New, G. Maunsell & Partners, London
BULLOCK La Canada
ERVIN, DOUG Belmont, CA
R.F. BESIER Old Saybrook CT

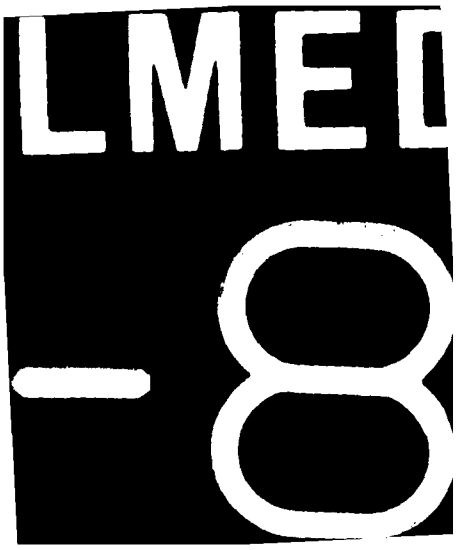
LMED
-8